Version of Record: https://www.sciencedirect.com/science/article/pii/S0022169417308016
Manuscript_60eb356b3f8973936e8b98f20baadfb6

Comparison of new generation low-complexity flood inundation mapping tools with a hydrodynamic model

Shahab Afshari[1], Ahmad A. Tavakoly[2], Adnan Rajib[3], Xing Zheng[4], Michael L. Follum[2], Ehsan Omranian[5], Balázs M. Fekete[6]

1. Department of Civil Engineering, The City College of New York, CUNY Environmental CrossRoads Initiative, CUNY CREST Institute, City University of New York, 160 Convent Ave, Marshak Rm #826, New York, NY 10031, USA
   Email: safshar00@citymail.cuny.edu

2. Coastal and Hydraulics Laboratory, U.S. Army Engineer Research and Development Center, 3909 Halls Ferry Road, Vicksburg, MS 39180, USA
   Emails: Ahmad.A.Tavakoly@erdc.dren.mil; michael.l.follum@usace.army.mil

3. Lyles School of Civil Engineering, Purdue University, 550 W Stadium Ave, West Lafayette, IN 47907, USA
   Email: adnanrajib@purdue.edu

4. Department of Civil, Architectural & Environmental Engineering, University of Texas at Austin; Austin, TX 78712, USA
   Email: zhengxing@utexas.edu

5. Department of Civil and Environmental Engineering, University of Texas at San Antonio, San Antonio, TX 78249, USA
   Email: SeyedEhsan.Omranian@utsa.edu

6. Department of Civil Engineering, The City College of New York, CUNY Environmental CrossRoads Initiative, CUNY CREST Institute, City University of New York, Steinman Hall Room #188, 160 Convent Avenue, New York, NY 10031, USA
   Email: bfekete@ccny.cuny.edu

Keywords:

Hyper-resolution modeling, AutoRoute, HAND, HEC-RAS 2D, multi-model comparison, National Water Model

Abstract:

The objective of this study is to compare two new generation low-complexity tools, AutoRoute and Height Above the Nearest Drainage (HAND), with a two-dimensional hydrodynamic model (Hydrologic Engineering Center-River Analysis System, HEC-RAS 2D). The assessment was conducted on two hydrologically different and geographically distant test-cases in the United States, including the 16,900 km^2 Cedar River (CR) watershed in Iowa and a 62 km^2 domain along the Black Warrior River (BWR) in Alabama. For BWR, twelve different configurations were set up for each of the models, including four different terrain setups (e.g. with and without channel bathymetry and a levee), and three flooding conditions representing moderate to extreme hazards at 10-, 100-, and 500-year return periods. For the CR watershed, models were compared with a simplistic terrain setup (without bathymetry and any form of hydraulic controls) and one flooding condition (100-year return period). Input streamflow forcing data representing these hypothetical events were constructed by applying a new fusion approach on National Water Model outputs. Simulated inundation extent and depth from AutoRoute, HAND, and HEC-RAS 2D were compared with one another and with the corresponding FEMA reference estimates. Irrespective of the configurations, the low-complexity models were able to produce inundation extents similar to HEC-RAS 2D, with AutoRoute showing slightly higher accuracy than the HAND model. Among four terrain setups, the one including both levee and channel bathymetry showed lowest fitness score on the spatial agreement of inundation extent, due to the weak physical representation of low-complexity models compared to a hydrodynamic model. For inundation depth, the low-complexity models showed an overestimating tendency, especially in the deeper segments of the channel. Based on such reasonably good prediction skills, low-complexity flood models can be considered as a

suitable alternative for fast predictions in large-scale hyper-resolution operational frameworks, without completely overriding hydrodynamic models' efficacy.

1. INTRODUCTION

With an increasing stress of climate and land use changes in recent times, flood events are becoming more frequent and perhaps more disastrous (Hirabayashi, et al. 2013). In the past 30 years, estimated costs of average annual flood damage is approximately $8 billion within the United States (US) (National Weather Service – Hydrologic Information Center, 2016). Accordingly, there is a growing interest in regional to continental scale high/hyper resolution flood forecasting and risk assessment across various parts of the globe (e.g. Alfieri et al., 2013; Bierkens et al., 2015; Paiva et al., 2011; Pappenberger et al., 2012; Winsemius et al., 2013; Wood et al., 2011). Maidment (2015) proposed a modeling architecture to forecast streamflow in 2.7 million river reaches across the continental US, which became operational in 2016 under the National Water Model (NWM) framework (http://water.noaa.gov/about/nwm). Despite these advancements, translating streamflow forecasts into time-varying flood inundation maps with reasonable accuracy and speed remains an outstanding concern.

Hydrologic models contain a rainfall-runoff estimator and a channel routing scheme, therefore, another model component is required to simulate the over-bank conditions (i.e. flood inundation). Many model applications for inundation mapping exist in literature (Table 1). Out of these alternatives, Hydrologic Engineering Center-River Analysis System (HEC-RAS), with 1D flow simulation functionality, has been the principal model used in US Federal Emergency Management Agency (FEMA)'s National Flood Insurance Program (FEMA, 2015) and National Oceanic and Atmospheric Administration (NOAA)'s Advanced Hydrologic Prediction Service

(NOAA, 2011). The ability of performing coupled 1D/2D analysis has been recently added to HEC-RAS (hereafter, HEC-RAS 2D; Table 1) which is still being tested under different geophysical settings. With a few exceptions of the LISFLOOD-FP model (e.g. Alfieri et al., 2014; Rajib et al., 2016; Schumann et al., 2013), most of the model applications listed in Table 1 are limited to small spatial scales over either a single river reach or a low-density river network.

Executing most of the hydraulic/hydrodynamic models requires modelers' intervention to provide substantial spatial details (e.g. channel and flood-plain cross-sections, optimum parameter values), which are often not readily available. Accordingly, the majority of these modeling packages come with a "black-box" configuration that can be executed only for research purposes in a stand-alone desktop environment (Kauffeldt et al., 2016; Néelz, 2009). These models also require considerable setup and computation time, especially with high resolution river networks. Accordingly, using a model that is as realistic as possible is not the panacea (Hunter et al., 2007); the choice should be balanced against several other considerations when it comes to the question of integration into a continental scale operational system such as the NWM.

Choice of a hydraulic/hydrodynamic model as component of a large scale framework is determined less by the superior model physics and more by its suitability to be executed in cyber infrastructures, computational overhead, interoperability with the driver hydrologic model, output retrieval, and visualization capabilities (Rajib et al., 2016). Being driven by such constraints, Follum (2012) introduced AutoRoute (Table 1) as a rapid tool to create flood inundation mapping over large scales. Using the simulated streamflow outputs from Tavakoly et al. (2017) as an input forcing to the AutoRoute, Follum et al. (2017) generated high resolution (~10 m) flood maps for the Midwest US (230,000 km^2) and the Mississippi Delta (109,500 km^2).

Despite such intensive application, computational overhead for executing AutoRoute was remarkably small. Liu et al. (2016) adopted the concept of Height Above the Nearest Drainage (HAND; Nobre et al., 2011; Rennó et al., 2008) and transformed 10 m National Elevation Dataset (NED) for the continental US into a HAND raster. This HAND raster shows the relative height of a given location above the nearest reach in the nationally mapped river network (National Hydrography Dataset Plus). Maidment et al. (2016) featured several case studies based upon the loose coupling of NWM streamflow outputs with this HAND raster to generate near real-time flood inundation maps. Considering these recent advancements, it is timely to examine whether fast-computing, "low-complexity" inundation mapping tools with simplified input requirements and process-representations can be preferred from an operational standpoint, particularly in time-limited emergency response scenarios, over computationally exhaustive, input intensive, physics based and presumably accurate hydraulic/hydrodynamic models.

Ability to capture natural floodplain processes and the influence of man-made control structures is different in each model. No model has the perfect realization of flooding; hence, simplification of the model physics may further undermine its already-limited ability. In this regard, a multi-model comparison can help measure relative accuracy of each model. Previous studies are heavily skewed towards the comparison of 1D versus 2D hydraulic/hydrodynamic models (e.g. Cook and Merwade, 2009; Alho and Aaltonen, 2008; Benjankar et al., 2014; Horrit and Bates, 2002; Leandro et al., 2009; Tayefi et al., 2007; Vojinovic and Tutulic, 2009). Several studies have compared different 2D models (e.g. Horritt and Bates, 2001; Vanderkimpen et al., 2009) or the same model under different configurations of topographic resolution and/or surface roughness (e.g. Bates et al., 2003; Cook and Merwade, 2009; Horritt and Bates, 2001b; Mason et al., 2003; Pappenberger et al., 2005). Effects of other geophysical and man-made attributes including channel bathymetry, levees, and bridges on model-simulated flood inundation has remained relatively unexplored (e.g. Cook and Merwade, 2009; Pappenberger et al., 2006).

The new-generation low-complexity inundation mapping tools, such as AutoRoute and HAND, have not been compared with each other, or with advanced hydrodynamic models (e.g. HEC-RAS 2D). Although AutoRoute was compared with reference inundation extents (Follum et al., 2017), HAND's efficacy is yet to be tested. This study, developed upon the preliminary work of Afshari et al. (2016), attempts to fill this gap with a view to provide a "practical, yet reliable" flood inundation modeling alternative to be coupled with continental scale hydrologic forecasting models. The main objective of this study is to evaluate the relative accuracy between AutoRoute, HAND, and HEC-RAS 2D for different magnitudes of flooding events, in terms of both inundation extents and depths. The Cedar River (CR) in Iowa and Black Warrior River (BWR) in Alabama in the US were considered as test-cases to represent two different spatial scales, terrain, land use and hydro-climatic conditions. For one of the test-cases (BWR), models are compared after incorporating geophysical and man-made attributes (e.g. channel bathymetry and levee) such that the resultant difference in the outcomes invoke avenues of future refinement in their current structures.

[TABLE 1]

2. METHODOLOGY

The assessment presented in this study is based upon 39 model configurations involving three models, three flood events, four terrain setups, and two test beds. Figure 1 summarizes the general design of this study, showing that each model (i.e. HEC-RAS 2D, AutoRoute, and HAND) was executed over the BWR test-case separately for three flood events (10-, 100-, and

500-year return period) and four different terrain setups (e.g. with and without channel bathymetry and levee). Concerning the much larger test-case (i.e. CR), only a single flood event (100-year return period) and terrain setup (without channel bathymetry and levee) were considered. The models were compared with one another for inundation extent and depth, separately in each of the terrain-flood configurations. In one of the configurations of BWR, FEMA estimated flood extents and depths were also used as a reference to compare with model simulations. All these configurations are summarized in Table 2. To keep the terminology obvious and self-explanatory, configurations were named in terms of the attributes in their respective terrain setups (e.g. NED, NED+Bathymetry, NED+Levee, NED+Bathymetry+Levee).

[FIGURE 1]

[TABLE 2]

2.1 Study Domains and Hydraulic Control Structures

Figure 2 illustrates the test-cases - a 16,900 km^2 Cedar River (CR) watershed in Iowa and a much smaller 62 km^2 area along the Black Warrior River (BWR) in Alabama in the US. The CR watershed stretches about 380 km in a mild/moderate terrain (~0.0001 m/m), from Mower County in Minnesota to a US Geological Survey (USGS) outlet in Cedar Rapids, Iowa (USGS 05464500). Along its way downstream, the main channel is fed by 11 major tributaries some of which are also divided into lower order upstream headwater reaches. The BWR domain stretches approximately 15 km through a moderate/slightly terrain (~0.0003 m/m) in Tuscaloosa county, Alabama with 15 adjoining tributaries. The river networks used for flood simulation in both cases were obtained from NHDPlus (McKay et al., 2012). The dominant land use in CR is agricultural, whereas the BWR domain used in this study is mostly an urban landscape with some forested areas.

CR is relatively a natural landscape with least obstruction by man-made hydraulic control structures. In contrast, the BWR domain has one levee and two lock/dams in the main channel (associated with two USGS gauge stations; Figure 2). The levee has been in operation since August 1999 (construction date) to reduce flooding damage in the city of Northport. According to the US Army Corps of Engineers National Levee Database, the approximate length and average crest elevation of the levee are 3.3 km and 47.5 m, respectively. The Oliver lock and dam is located at the outlet of the study domain (USGS 02465000), whereas the Holt lock and dam (USGS 02462961) defines the upstream boundary location for the main channel. Flood inundation is influenced by these dams/levees due to their flow regulatory role and to possible backwater effects during extreme events. Incorporation of these man-made control structures, even in their simplest forms, can supplement the limited hydrodynamic simulation capacity of an inundation mapping tool.

[FIGURE 2]

2.2. Model Inputs

To enable an even assessment, the forcing data (i.e. input streamflow), topographic resolution, land cover classification, and the values of channel/surface roughness parameters were kept identical when the models were compared under the same configuration. The following sub-sections describe the model setups, including the sources of these input data and details on how they were processed for this study.

2.2.1 Construction of Input Streamflow Data

The specific flood magnitudes used for model simulation for this study are not actual events. The representative streamflow data to force the inundation models were constructed while maintaining the hydrologic "connectivity" of the river network and therefore accounting for the contribution of tributaries. For instance, difference between monthly mean downstream and upstream streamflow in the BWR domain implies higher values in the downstream station 87% of the time (Figure 3a). Figure 3b, comparing daily streamflow data at the upstream and downstream gauge stations for 19 peak flow events during a past 40-year period (1976-2014), also validates this notion. These findings help to realize two critical factors regarding the "connectivity" aspect mentioned above. First, amplification of flood magnitude while proceeding towards the outlet was due to the lateral flows from the tributaries; attenuation of flood peak by some diffusion effects can be considered negligible (discussed further in a later section). Secondly, the flood peaks in the tributaries occurred at the same time as in the main channel. These data-driven assessments justified the approach adopted here to determine the input streamflow forcing data for the inundation models.

[FIGURE 3]

In this study, input streamflow data for the three hypothetical flood events (10-, 100-, and 500-year return periods) were constructed by fusing NWM simulated outputs with USGS and FEMA estimates. Simulated hourly streamflow in all the associated NHDPlus reaches were obtained from a pre-operational offline repository of the NWM (personal communications with the NOAA National Water Center, Alabama) for a recent flooding event in respective study domains (September 25 – October 1, 2016 in CR (USGS, 2010) and December 24 – 31, 2015 in BWR (USGS, 2007)). Like other hydrologic models, NWM outputs have some discrepancies relative to the observed data (Figure 4). Since the use of NWM in this study was kept limited only to ensure hydrologic connectivity of river network, bias in its streamflow simulations did not affect the "relative accuracy" of the inundation models. Hence, further diagnostic evaluation of NWM's performance was not included here.

Based on the statistical analyses of long-term observations at the outlet of BWR, peak flow values for different return periods were estimated by USGS (2007). Accordingly, an event-specific scaling factor was calculated for the outlet of BWR, being defined as the ratio of corresponding USGS estimated magnitude and the NWM peak flow (USGS 02462951; Figure 4). For all other NHDPlus reaches including the main channel's upstream boundary location in BWR, respective NWM streamflow hydrographs were multiplied by the outlet's event-specific scaling factor to obtain three different sets of input forcing data. Similar approach was followed for CR except it was kept limited only for a 100-year flood event. CR being a much larger domain with densified gauge network, calculation of scaling factor for this case involved using USGS estimated peak flow at 14 upstream gauge stations (USGS, 2010) in addition to that at the outlet. For those reaches in CR with no USGS estimate, the nearest downstream station was selected for scaling purposes. FEMA (2008, 2010, 2013, 2014) also estimates peak flows for different return periods leveraging some field-studies and local expertise; however, such studies were available for five reaches in BWR and 16 reaches in CR (dashed lines in Figure 6). The FEMA suggested values were used in scaling factor calculation instead of USGS estimates, wherever seemed appropriate (i.e. specific reaches and flood return periods, depending on availability). Effect of these scaling factors on the constructed input streamflow are presented in Figure 5 in terms of relative channel thickness.

[FIGURE 4]

[FIGURE 5]

2.2.2. Inclusion of Floodplain Features

As summarized in Table 2, the terrain setups used for flood modeling in BWR include: (1) NED without channel bathymetry or levee (NED), (2) NED with channel bathymetry

(NED+Bathymetry), (3) NED with levee (NED+Levee), and (4) NED with both channel bathymetry and levee (NED+Bathymetry+Levee). However, flood modeling for CR is conducted only with a single terrain setup based on NED (without channel bathymetry or levee), considering its large spatial extent (16,900 km^2 compared to BWR's 62 km^2), lack of continuous bathymetry data and least hydraulic controls. The spatial resolution of NED was kept the same (10m) in every case. Hence, plausible differences in simulated inundation depth and extent while using these different terrain setups evolve solely from the respective ability of the models to capture floodplain hydrodynamics. Although the fourth terrain setup (i.e. NED+Bathymetry+Levee) is the best case to closely represent river corridor/floodplain, others help to create insights on the sensitivity of a model to particular floodplain feature(s).

The 10 m resolution of NED is not fine enough to identify abrupt topographical variability (e.g. height, width, and location of a levee, shape and thalweg of a channel), let alone the persistent inaccuracy that might have induced from the acquisition of elevation data and associated interpolation techniques. Use of Light Detection and Ranging (LiDAR) topography data significantly improves detection of land surface features such as levee, but its inability to "see through" water surface and capture channel bathymetry is not unknown (Cook and Merwade, 2009). In case of BWR, limited information on the longitudinal/cross-sectional dimensions and changes in elevation along the levee was obtained from a design-inventory of the US Army Corps of Engineers (USACE, 2014), part of which were tentatively validated by the authors in a non-exhaustive field survey using ground global positioning system (GPS) equipment. Furthermore, the main channel's water surface and bed elevation data were obtained from another field-campaign (obtained from the USACE Tuscaloosa Field Office), at a spatial resolution of 2-10 m along and across the channel. These are point elevation data, which were transformed into raster format to mosaic with the 10 m NED, producing the aforementioned terrain setups. Figure 6 shows the difference between the NED and NED+Bathymetry+Levee setups along a cross-section and a longitudinal section of the main channel. The effect of the dam/locks was implicitly incorporated in the streamflow data (section 2.2.1).

[FIGURE 6]

2.2.3. Land Cover and Surface/Channel Roughness

A common feature in HEC-RAS 2D and AutoRoute (also HAND, with some exceptions) is the provision of spatially distributed values of surface and/or channel roughness parameters. In this study, the same set of roughness values was used in each of the inundation models. The 2011 National Land Cover Database (NLCD 2011; Homer et al., 2015) at a 30 m spatial resolution is selected as the input land use data for both test-cases (e.g. highlighted in Figure 7a as an example from BWR). Depending on the respective land use class, a separate lookup table linked each grid cell of NLCD 2011 with a representative value of Manning's roughness coefficient *(n)*. Manning's *n* values were selected based upon the suggestions from Moors (2011); however, the "low roughness" category was used considering the recommendation by Follum et al., (2017). All the 30 m NLCD grid-cells classified as 'open water' basically represent the river network, hence, they were assigned the roughness value of a natural channel (n = 0.03). Unlike the HEC-RAS 2D and AutoRoute models, HAND does not require assigning *n* for the land surface. The current version of HAND only uses channel *n*, which was kept consistent with the other two models to enable an even comparison.

[FIGURE 7]

2.3. Flood Inundation Modeling

2.3.1. Hydrodynamic Model: HEC-RAS 2D

Hydrologic input to HEC-RAS 2D refers to the streamflow hydrographs (time-series) for each of the NHDPlus reaches involved and a streamflow-stage rating curve at the outlet location. Geospatial inputs include: (1) terrain (topography data) and (2) spatially distributed (gridded) surface/channel Manning's *n*. The model solves a 2D unsteady flow equation at hourly resolution using a diffusive wave approach. Although HEC-RAS 2D can also employ a "full momentum" approach (the Saint Venant equation), it was avoided in this study as it does not produce substantial differences in simulated inundation in a fairly uniform terrain like BWR or CR. Despite the relatively intensive computational demand, application of the Saint Venant equation in HEC-RAS 2D would be more useful in simulating critical scenarios such as levee breach and design of hydraulic structures. The simulation was performed on a heterogeneous mesh, simultaneously having structured and un-structured cells (e.g. the mesh highlighted in Figure 7). Abrupt changes in the terrain (e.g. river bank, levee) are delineated by "breaklines" and un-structured cells (up to nine faces and with different sizes), while square cells (25 m) are nested on the other parts of the landscape. Weighted average of elevation and roughness values respectively from all intersecting/encompassing cells of the 10 m terrain and 30 m roughness grid (NLCD, being linked with the lookup table) were "poured" on to a model cell regardless of its size/shape. In addition to capturing topographic details as precisely (un-structured cells) and parsimoniously (square cells) as possible, faces of these model cells work as "virtual cross-sections" that regulate the propagation of flood wave. Although such a detailed model setup would enable enhanced simulation of floodplain/channel's response in flooding conditions, it requires substantial intervention from the modelers. Outputs from HEC-RAS 2D are the time-varying flood inundation extents and depths out of which only those at the time-stamp of peak flow were extracted for comparison purposes. Running time is highly dependent on the amount of physical details imparted into the model (e.g. mesh resolution, number of boundary conditions).

2.3.2. Low-complexity Model: AutoRoute

Unlike HEC-RAS 2D, AutoRoute uses peak flow (not the time-series/hydrograph) at each NHDPlus reach. Other inputs to AutoRoute, including topography data and distributed surface/channel roughness values, were the same as those used in HEC-RAS 2D. Assuming 1D steady-state flow, AutoRoute uses Manning's equation to calculate the normal flow depth over a high-density number of cross-sections, while the cross-section geometry and channel slope were automatically generated from topography data. Flood depth and inundation maps were simulated using a volume-fill numerical method at each cross-section. Follum et al. (2017) provided more details on the setup rubrics and computational techniques of AutoRoute. Output from AutoRoute was a static set of inundation extent and depth, corresponding to the peak flow used to force the model (for each of the specific flood events; Table 2). Although streamflow and other input data for AutoRoute were manually processed in this study, supplementary tools have been developed for automatic pre-processing to enable its execution in an operational setting (Snow, 2016; AutoRoutePy: 2.1.0). It should be noted that AutoRoute is currently closed-source at the request of one of our Military sponsors but may soon be open source. Due to this uncertainty, the paper does not state whether it is open source. The AutoRoute executable is publically available by sending an access request to Michael Follum (Michael.L.Follum@erdc.dren.mil)

2.3.3. Low-complexity Model: HAND

HAND is a hydrological terrain analysis approach, which has been tested for reasonable functionality in producing flood inundation maps (Rodda 2005; Rennó et al., 2008; Nobre et al., 2016). In this approach, vertical distance between a grid-cell in topography data and the nearest cell along a stream that it drains into defines the "HAND value". All cells on the landscape that have a HAND value smaller than the specified stage (water level) are treated as inundated. HAND is entirely raster-based and defines the inundated zone by a corresponding river segment. Therefore, it does not require the creation of cross sections. A user-friendly, seamless workflow for the HAND model is currently under development, however, an executable prototype framework for US watersheds can be supported by Xing Zheng (zhengxing@utexas.edu).

In this study, 10 m HAND rasters were created with different terrain setups (four rasters for BWR and one for CR; Table 1), each with respect to the NHDPlus river network (e.g. Liu et al., 2016). These HAND rasters were then used to estimate stage height - channel hydraulic geometry relationships for each of the reaches (e.g. Zheng et al., 2016). Taking these relationships, estimated channel length and average slope from the NHDPlus database, and predefined channel roughness value (section 2.2.3), Manning's equation was applied to generate streamflow-stage rating curves for all the reaches. Using these rating curves, input peak flow corresponding to a given return period was converted into a stage height. Finally, the HAND raster was used to create the inundation extents at these particular stage heights.

2.4. Model Comparison Metrics

Quantifying the differences in inundation extents and depths between two flood models, and between flood models and the reference (e.g. FEMA in BWR case study), needs a mathematical scheme. For the comparison of inundation extents, an error matrix (e.g. Congalton and Green, 1999) was developed (Figure 8) using which Kappa-statistic and Fitness-statistic (being denoted as κ and $\mathcal{F}$, respectively) (Yu and Lane, 2006) were calculated to measure the degree of agreement or disagreement between two flood maps. The κ statistic is a ratio between the actual agreement (indicated by major diagonal of the error matrix) of the two models and the chance of agreement (expressed through marginal rows and columns of the error matrix) (Equation 1). Hence, an impressive κ value is possible even with fewer matching wet cells. For instance, in the case of flood events, where there are few number of conforming wet cells (i.e. $n_{w1,w2}$) relative to the large number of conforming dry cells (i.e. $n_{d1,d2}$), κ might be close to 1.

$$\kappa = \frac{n.(n_{w1,w2} + n_{d1,d2}) - (n_{w1+d1,w2} n_{w1,w2+d2} + n_{w1+d1,d2} n_{d1,w2+d2})}{n^2 - (n_{w1+d1,w2} n_{w1,w2+d2} + n_{w1+d1,d2} n_{d1,w2+d2})} \qquad (1)$$

$\mathcal{F}$ reduces bias into results since it only considers the number of conforming wet cells predicted by both flood models (Equation 2):

$$\mathcal{F} = \frac{n_{w1,w2}}{n_{w1,w2+d2} + n_{w1+d1,w2} - n_{w1,w2}} \qquad (2)$$

where n is total number of cells; $n_{w1,w2}$ is number of cells predicted wet by both inundation models; $n_{d1,d2}$ is number of cells predicted dry by both inundation models; $n_{d1,w2}$is number of cells predicted dry by model 1 but as wet by model 2; $n_{w1,d2}$ is number of cells predicted wet by model 1 but as dry by model 2; $n_{w1,w2+d2}$ is number of cells where model 1 predicted them as wet while model 2 predicted either wet or dry; $n_{w1+d1,d2}$ is number of cells where model 2 predicted them as dry while model 1 predicted either wet or dry; $n_{d1,w2+d2}$ and $n_{w1+d1,w2}$ are being read in same fashion to $n_{w1,w2+d2}$ and $n_{w1+d1,d2}$ respectively. Both of these inundation metrics range from 0 to 1 denoting lowest and highest conformity, respectively.

[FIGURE 8]

Flood inundation depths were compared by calculating Mean Difference (MD) and Root Mean Squared Difference (RMSD) between the simulated outputs from two models or between a model and a reference. Both MD and RMSD were computed based upon an average of cell-by-cell difference and squared difference of two flood inundation depth layers:

$$\mathrm{MD} = \frac{1}{\mathbf{N}} \sum_{\mathbf{i=1}}^{\mathbf{N}} (Z_{1,i} - Z_{2,i}) \tag{3}$$

$$\mathrm{RMSD} = \frac{1}{\mathbf{N}} \sqrt{\sum_{\mathbf{i=1}}^{\mathbf{N}} (Z_{1,i} - Z_{2,i})^{\mathbf{2}}} \tag{4}$$

where N is total number of raster cells; $Z_{1,i}$ and $Z_{2,i}$ are depth values simulated respectively by flood model 1 and 2 at the i^{th} cell. MD and RMSD need careful interpretation, if used together. Lower MD may not always come with lower RMSD. For a constant MD, RMSD can increase as the variance associated with the frequency distribution of error magnitudes also increases. Accordingly, the sole purpose of MD was kept limited in this study only to evaluate a model's general overestimating/underestimating tendency with respect to the other model or the FEMA reference, while RMSD should be seen as a metric of models' relative accuracy.

An R code was developed to perform one-to-one comparison of model products (i.e. flood inundation extent and depth) with the option of calculating a suite of conformity statistics as described above (Afshari, 2016, 2017).

3. RESULTS AND DISCUSSION

This section presents the outcome of the study from three aspects: (1) comparison among models for flood extents, (2) comparison among models for flood depths, and (3) comparison of the models with FEMA flood estimates for a specific flood magnitude (only for BWR test-case).

3.1 Comparison of Flood Extents

3.1.1. Inter-comparison of Models for Inundation Extent

For the CR test-case, HEC-RAS 2D, AutoRoute, and HAND were compared for flood extent and depth only for a 100-year flood. Only the most simplistic terrain setup, without channel bathymetry or other possible floodplain features, was considered in this case, with a view to have a closer look on some critical aspects where flood models usually struggle over large spatial scales. Specifically, the model comparisons on CR solicited a general assessment whether low-complexity models "behave" in the same manner as the hydrodynamic model regardless of meandering main channel segments, confluence, and lower order headwater reaches.

In general, HEC-RAS-2D resulted in notably larger inundated area compared to AutoRoute and HAND. Across the entire test-case, differences in inundated area between HEC-RAS 2D and AutoRoute and between HEC-RAS 2D and HAND were respectively 382 and 229 km^2, which made HAND simulations closer to HEC-RAS 2D. Although HAND inundated a slightly larger area than AutoRoute, spatial patterns of their respective inundation were nearly identical in each of the four cases (A1 – A4) highlighted in Figure 9. This was also evident from κ and $\mathcal{F}$ as both of the low-complexity models basically showed the same fitness scores against the inundation extent of HEC-RAS 2D.

As indicated in section 2.4, concurrent occurrence of high κ and low $\mathcal{F}$ is quite possible. κ shows conformity in the number and location of dry cells between the models, not the conformity of their actual inundated extents. Still, a κ value as high as one in CR strongly suggests that the low-complexity models function very reasonably. Concerning the actual match of wet cells (i.e. inundation), obtaining a lower $\mathcal{F}$ value could be potentially misinterpreted. It is likely for an uncalibrated low-complexity model to show lower $\mathcal{F}$ values against a much more detailed hydrodynamic model, especially when executed over a large area such as the CR. Nevertheless, a relatively low fitness of inundated boundaries ($\mathcal{F}$ values ~ 0.5 in Figure 9) cannot be undermined as the typical disagreement between the two models; $\mathcal{F}$ values were found substantially higher when looked specifically into A3 or A4 portions of the test-case. This could also be supported by visually assessing the highlighted portions in CR (Figure 9). For example, with respect to HEC-RAS 2D, low-complexity models showed large differences along the main channel and its confluences with the tributaries (A1 and A2 in Figure 9); however, such difference was found minimal in the lower order less-meandering reaches in the upstream headwater catchments (A3 and A4 in Figure 9).

[FIGURE 9]

A small-scale yet more comprehensive comparison was deduced from the BWR test-case focusing more on the models' response to floodplain features such as bathymetry and levee. HEC-RAS 2D, AutoRoute, and HAND were compared for flood extent using 10-, 100-, and 500-year events, and for four different terrain setups (Figures 10-12). The results suggest expansion of inundation extents when the return period increased from 10-year to 500-year for all the models; however, the percent change of extent between return periods was not identical when models were compared with one another. For four terrain setups in HEC-RAS 2D, the average expansion of the flood extent was 25% and 11% from 10-year to 100-year and from 100-year to 500-year flood events, respectively. Although AutoRoute is not a hydrodynamic model, it closely mimics HEC-RAS 2D in most parts of the study region. AutoRoute showed an average expansion of flood extent by 20% between 10-year and 100-year and 10% between 100-year and 500-year event simulations. Compared to HEC-RAS 2D, a limitation in AutoRoute is the absence of any downstream boundary condition (dam/lock in BWR main channel). Accordingly, difference in inundation extents between HEC-RAS 2D and AutoRoute, as observed in the first column of Figures 10-12, might be due to AutoRoute's inability to capture the possible "backwater effect" during the higher magnitude events. Similar to AutoRoute, representation of the wave propagation (e.g. backwater effect) is a limitation in HAND. Moreover, HAND showed flooding in physically implausible locations which have similar elevation difference with respect to the nearest reach (the main channel in this case). As a result, HAND produced larger inundated area than AutoRoute when both were compared against HEC-RAS 2D. This is similar to what was observed in the case of CR test-case. For BWR, HAND showed an average expansion of flood extent by 31% between 10-year and 100-year events and 5% between 100-year and 500-year flood events. Among all the configurations, regardless of terrain setup or flood event, AutoRoute invariably showed better performance than HAND in capturing the inundation extent of BWR in terms of κ and $\mathcal{F}$.

[FIGURE 10]

[FIGURE 11]

[FIGURE 12]

3.1.2. Effect of Terrain Setups on Inundation Extent

Depending on the model, effects of floodplain attributes (e.g. levee and bathymetry) on the simulated inundation extents can be noticeably different. In the BWR test-case, HEC-RAS 2D and AutoRoute showed reasonably good agreement irrespective of return periods, even without the incorporation of channel bathymetry or levee (e.g. $\mathcal{F}$ = 0.71-0.75). Incorporation of the levee (NED+Levee setup) could not mitigate HAND's overestimating tendency. As the relative elevation with respect to the nearest channel is a key determinant for HAND, the model essentially over-laid the same “over-bank” stage from the particular channel segment on both sides of the levee. In reality, spatial orientation of the levee acts as a confinement and thus controls the movement of flood wave, which was relatively well-captured by HEC-RAS 2D and AutoRoute.

Both AutoRoute and HAND showed prominent overestimation of inundation extents relative to HEC-RAS 2D throughout the entire length of the main channel once bathymetry was incorporated in the terrain. More specifically, HEC-RAS 2D tended to retain more “within-bank” water because of the deeper and wider channel in the NED+Bathymetry and NED+Bathymetry+Levee setups. This phenomenon was vivid for 10-year and 100-year events (Figures 10 and 11, respectively). Accordingly, the best model conformity in the NED+Levee setup (i.e. highest κ and $\mathcal{F}$) does not necessarily mean that model simulated inundation extents were more accurate in this particular terrain setup. Considering NED+Bathymetry+Levee to be a relatively better realization of the floodplain compared to other terrain setups, raises questions to why AutoRoute and HAND are unable to leverage from this terrain setup and remains as an outstanding question needing further investigation looking into possible scopes of model re-conceptualization. Regardless, the NED+Bathymetry+Levee setup exemplified a crucial aspect regarding the effect of bathymetry in case of an extreme flood event (e.g. 500-year; Figure 12). In that case, flood water was found to have over-topped the levee in the NED+Levee setup in all the models, but HEC-RAS 2D and AutoRoute did not allow over-topping when bathymetry was included in the model configuration (NED+Bathymetry+Levee). This is a clear example of bathymetry being a controlling factor that determines the shape of flood inundation map, except in HAND. Here as well, AutoRoute has relatively better capability than HAND, at least with current versions.

3.2. Comparison of Flood Depth

Inter-comparison of simulated inundation depths (as raster data layers) was carried out only for the 100-year flood event in both CR and BWR test-cases. The common (intersecting) area of the inundation extents generated by two particular models was taken as the boundary within which flood depth comparison was carried out.

3.2.1. Inter-comparison of Models for Inundation Depth

Figures 13 demonstrates the comparison among HEC-RAS 2D, AutoRoute, and HAND for inundation depth in CR, only for a 100-year flood event. Over the entire stream network of CR, HEC-RAS 2D produced 11-16 m (MD) deeper floods than AutoRoute and HAND, which is in line with its overestimation of inundation extent (Figure 9). Similarly, both low-complexity models had minimal difference (< 2 m) in their respective simulated depths. However, HAND produced a slightly deeper flood than AutoRoute as evident from MD, making the models' behavior coherent with what was depicted in Figure 9 for their flood extent simulation. Furthermore, HAND simulated depth had an RMSD of ~9 m against HEC-RAS 2D, contrary to AutoRoute's 17 m. This led to the notion that HAND simulations were relatively more consistent with HEC-RAS 2D, at least in CR. The meandering main channel (a near-outlet location) and confluences (A1 and A2) again appeared to be the hot-spots where both AutoRoute and HAND struggled, but their performance to simulate flood depth is equivalent to HEC-RAS 2D in the case of less-meandering upstream headwater catchments (A3 and A4).

For the BWR test-case, inundation depth of a 100-year flood event for all terrain setups showed an average MD of 0.8 m between HEC-RAS 2D and AutoRoute, with AutoRoute resulting in deeper inundation (Figure 14). HAND produced even deeper inundation as its average MD from HEC-RAS 2D was about 4 m. In general, both AutoRoute and HAND overestimated depth with respect to HEC-RAS 2D which is opposite to what was detected from the CR test-case. Analogous to the results shown for inundation extent (section 3.1.1), bias in depth simulation was nearly 50% less in AutoRoute than that in HAND in terms of their RMSD against HEC-RAS 2D. Variability of depth along the main channel was found to be more consistent between HEC-RAS 2D and AutoRoute in most parts of the river network. On the other hand, variability of depth simulated by HAND was relatively more erratic (hence, may not be realistic).

In the 16,900 km^2, 380 km long CR test-case, the low-complexity models generally showed an underestimating tendency to simulate inundation extent and depth, while HAND produced closer results to the HEC-RAS 2D model. The opposite was found in the 62 km^2, 15 km long BWR test-case with AutoRoute being relatively accurate with respect to HEC-RAS 2D. Here, the scale is important. For example, there are specific locations with short reach segments within CR, where the low-complexity models behaved similarly as in the case of BWR. Hence, the outcome from the BWR test-case, showing AutoRoute and HAND overestimating inundation extent and depth is not an anomaly, rather it is a very likely subset of possibilities that might have happened if a much larger domain along the Black Warrior River system was modeled in this study.

[FIGURE 13]

[FIGURE 14]

It could seem ambiguous why AutoRoute differs from HAND even though both are based on Manning's equation. Despite using Manning's equation, the procedure of generating flood maps is not similar in these models. AutoRoute generates flood inundation map (extent) and depth "vertically", whereas HAND does it "laterally". More specifically, AutoRoute automatically generates cross-sections, calculates flood extent for user-defined input streamflow values using iterative calculation of flow for every cross section (Follum et al., 2017). The depth is incrementally increased from the lowest point in the reach until the calculated streamflow from Manning's equation matches the input streamflow. In the HAND method, first a synthetic stage-discharge rating curve is generated for each NHDPlus reach using Manning's equation. For a user-defined input streamflow, a corresponding depth value is extracted from such a rating curve (Liu et al., 2016). All cells on the landscape with a HAND value smaller than this depth will be considered as inundated. Hence, this method does not require cross sections and it also does not have the direct incorporation of streamflow as in AutoRoute. In this way, use of Manning's equation in HAND does not produce similar results as in the AutoRoute model.

3.2.2. Effect of Terrain Setups on Inundation Depth

Similar to the multi-model multi-terrain assessment of inundation extent (section 3.1.2), simulated flood depth in the BWR test-case was also evaluated under four different terrain setups. When the models were configured with the simplest terrain setups, NED and NED+Levee, AutoRoute showed the least bias for flood depth simulation with respect to HEC-RAS 2D (relevant RMSD values for a 100-year event; Figure 14). Once bathymetry was incorporated, AutoRoute showed signs of discrepancy as the RMSD value relative to HEC-RAS 2D increased by more than 1 m. Exactly similar phenomenon was observed in the case of HAND when it was compared with HEC-RAS 2D (middle column of Figure 14). What is more interesting here is the remarkable similarity between AutoRoute and HAND pertaining to their behavior in depth simulation in certain segments of the main channel. Contrary to their general depth overestimating tendency relative to HEC-RAS 2D, both AutoRoute and HAND distinctly underestimated flood inundation depth in the middle and near-outlet locations in the “bathymetry-informed” terrain setups. Even when comparing HAND and AutoRoute, NED+Bathymetry+Levee showed the highest RMSD (7.64 m) out of all terrain setups being modeled here. Overall, this analysis resonates the insensitivity of these low-complexity flood models to cope with hydrodynamics, especially in meandering portions of the channel (middle section), the deeper portions in the near-outlet location with a navigational dam/lock, and nearby levee, not to mention their inability to capture back water effects. However, in such cases, AutoRoute seemed to be better-equipped than HAND, similar to the findings highlighted in section 3.1.2 for simulation of inundation extent.

3.3 Evaluation of Model Performance with FEMA Reference Estimates

Figure 15 compares model simulated inundation extent and depth for a 100-year flood event with the corresponding FEMA estimates. This assessment was kept limited only on BWR test-case as it has nearly all real-life examples of floodplain features that often make flood models under-perform. The FEMA flood map (i.e. inundation extent) was obtained via Flood Map Service Center (https://msc.fema.gov/portal), which is the official public source for sharing flood hazard information in terms of flood maps and other related products. The technical information from FEMA-Coordinated Needs Management Strategy (FEMA-CNMS) platform as well as FEMA’s R4 Regional Service Center assured that channel bathymetry was not considered for developing the 100-year flood hazard map in BWR. Another considerable factor was that FEMA estimates on flood extent and depth were available only for the downstream portion of BWR encompassing the levee. Hence, comparing the models with FEMA estimates seemed justified only for the "NED+Levee" terrain setup. Clearly, HEC-RAS 2D had the most conformity with FEMA estimates for flood extent (Figure 15). The κ and $\mathcal{F}$ scores were 0.94 and 0.74, respectively, for the HEC-RAS 2D versus FEMA case. These scores were 0.93 and 0.69 when the flood extent generated by AutoRoute was compared with the FEMA flood map. Comparison of the HAND and FEMA flood extents resulted in κ and $\mathcal{F}$ equal to 0.88 and 0.53, respectively. In case of flood depths, HEC-RAS 2D quite expectedly produced the lowest RMSD (2.23 m), while AutoRoute and HAND had an RMSD of 3.33 m and 5.36 m, respectively. The average of differences (MD) for FEMA flood depth against HEC-RAS 2D, AutoRoute, and HAND were respectively captured as -1.55, 0.37, and -1.27 m. The MD values show that AutoRoute and FEMA are relatively similar whereas HAND and HEC-RAS 2D underestimate the flood depth derived by FEMA. AutoRoute and FEMA both use similar methods (Manning equation) which can explain similarity of MD values. Since HEC-RAS 2D applies the unsteady hydrodynamic (2D Diffusion Wave) equation, it might produce lower depth compared to the steady state approach. This is due to the fact that the unsteady state equation factors in additional physically-based terms may lower the simulated water stages compared to ones estimated by steady state approach (being applied in FEMA and AutoRoute). HAND model shows overestimation of depth at upstream and abruptly underestimation of depth when a levee exists (Figure 15) which resulted in overall underestimation of depth with this model compared to the FEMA model.

[FIGURE 15]

4. CONCLUSION

This paper inaugurates a new line of research to compare the sensitivity and suitability of new-generation low-complexity flood models. With increasing flood hazards across the world, it has been a burning question whether it is sustainable to employ computationally intensive yet supposedly better hydrodynamic models in large-scale hyper-resolution operational flood simulation. Against such concern, a few models were developed with the fast-computing capability due to simplified input requirements and process-representations yet reasonably good in terms of prediction accuracy. This paper compares two such genres of recently-developed inundation models: a hydrodynamic model (i.e. HEC-RAS 2D) and two low-complexity models (i.e. AutoRoute and HAND). To the best of authors' knowledge, this is also the first flood inundation assessment using United States National Water Model (NWM) streamflow data.

The assessment presented in this study is based upon 39 model configurations involving three models, three flood events, four terrain setups, and two test beds. Models were compared for two hydrologically different and geographically distant test-cases in the United States, including the 16,900 km^2 Cedar River (CR) watershed in state of Iowa and a 62 km^2 domain along the Black Warrior River (BWR) in state of Alabama. Model comparison in CR was conducted using only one terrain setup (i.e. National Elevation Dataset, NED) and a 100-year flood event, with a view to focus on issues such as meandering channel segments and confluences where flood models usually struggle. A much more detailed analysis was conducted over the BWR test-case including moderate to extreme flood events at 10-, 100-, and 500-year return periods and various terrain setups with levee and/or bathymetry. The streamflow time-series from the pre-operational offline repository of the NWM were used and processed to define inflow boundary conditions of the flood events for all NHDPlus reaches in the test-cases.

Results showed HEC-RAS 2D, AutoRoute, and HAND can be ranked according to their model complexity and computational capability. HEC-RAS 2D is the most and HAND is the least complex model. The HAND model results were relatively closer to HEC-RAS 2D compared to the AutoRoute model for depth and flood extent in the CR study domain. However, in the relatively less meandering upstream headwater rivers, both AutoRoute and HAND behaved the same as HEC-RAS 2D. This can be attributed to the nature of low complexity models, their inherent capabilities, and limitation, which might perform well in simple landscape. Results also showed that in complex conditions such as meandering main channels and confluences, low complexity models struggle to generate results that are comparable to the HEC-RAS 2D model. In the BWR test-case, AutoRoute generally outperformed HAND when compared to the HEC-RAS 2D model when hydraulic controls such as dams and levee were incorporated. One should note that both low complexity models demonstrated identical spatial variation of flood extents, despite the difference between magnitudes of flood extent or flood depth. Considering model performance with different terrain setups, HEC-RAS 2D and AutoRoute models showed similar results for the NED+Levee terrain setup with HAND showing some inconsistency in capturing the effect of any abrupt geophysical variation (e.g. enforced by the levee). Contrarily, terrain setups with bathymetry (e.g. the NED+Bathymetry+Levee terrain setup) showed prominent discrepancy between the low-complexity models in comparison with the hydrodynamic model. This behavior is speculated to be driven by assimilation of different river bed-slope at each NHDPlus reach (i.e. channels with bathymetry versus channels having a "flat-bed" as given by NED), and thus, resultant change in the vertical distance between a given cell on the floodplain and the nearest channel cell that it drains into. In general, the low-complexity models should be set up with caution in flat and densely urbanized zones (e.g. in the downstream regions of the BWR study domain) since they do not capture the backwater effects created by existing hydraulic structures. Further study in different climate and land use conditions would be helpful to validate these findings.

Despite the generally favorable results obtained in this study, it is up to the users discretion whether a low-complexity flood inundation mapping tool should be preferred or complex hydrodynamic models. As a near future application, low complexity models can provide a rapid, first order estimate of flood inundation to prioritize evacuation areas during severe flood events. Furthermore, the combination of both types of modeling approaches can be considered. For instance, the low complexity models can be used for flood mapping at the regional scale with a nested high-fidelity model at the local scale where anthropogenic effects and topographic conditions need to be considered. Results of this study showed that low-complexity tools can have “nearly equal applicability” while retaining the value of complex hydrodynamic models. This notion is based upon a trade-off between highest possible accuracy and computational efficiency, which is permissible for operational needs. Moreover, to provide operational hydrologic support in geographic areas where hydrologic data is sparse, and because the assessments provided are time critical, alternative approaches can be employed to develop terrain and bathymetry data. For instance, idealized power-law hydraulic geometries which are derived based on bank-full hydraulics of the channel can be established given measured basic hydraulics (i.e. discharge, water surface width, average depth, and average velocity) and applied to generate asymptotic forms of the channel bed geometry. Application and deployment of this methodology in the low complexity models can be considered as a far future work.

ACKNOWLEDGMENTS

This work was conducted in a continuing effort to complete the multi-model comparison study which was initiated at the 2016 National Water Center Innovators Program supported by the Consortium of Universities for the Advancement of Hydrologic Science, Inc. (CUAHSI) and the National Oceanic and Atmospheric Administration. The authors would like to appreciate the support of those involved in the coordination and execution of this project including Dr. David Maidment, Dr. Sagy Cohen, Dr. Sarah Praskievicz, Dr. Edward P. Clark, Mr. Alan Snow, Ms. Elissa Yeates, and Ms. Kayla (Hudson) Cotterman. This project was partially funded by Deputy Assistant Secretary of the Army for Research and Technology through the Engineer Research and Development Center's Military Engineering applied research work package title Austere Entry and was supported exclusively by internal funding from The City College of New York including the Andrew S. Grove Endowment.

REFERENCES

Afshari, S. 2016. "R, Repository: https://github.com/sha17hab/Flood-Inundation-Mapping-and-Comparison-of-Two-Models." *License: GNU GENERAL PUBLIC LICENSE.* http://doi.org/10.5281/zenodo.221189.

Afshari, S. 2017. "R, Repository: https://github.com/sha17hab/Working-With-NWM-NetCDF-Products/tree/V.1.1." *License: GNU GENERAL PUBLIC LICENSE.* http://doi.org/10.5281/zenodo.893563.

Afshari, S., E. Omranian, and D. Feng. 2016. *Relative Sensitivity of Flood Inundation Extent by Different Physical and Semi-empirical Models. In Maidment et al. (Eds.).* Technical

Report 13, National Water Center Innovators Program Summer Institute Report 2016, Consortium of Universities for the Advancement of Hydrologic Science Inc. (CUAHSI), USA, 19-24.

Alfieri, L., P. Burek, E. Dutra, B. Krzeminski, D. Muraro, J. Thielen, and F Pappenberger. 2013. "GloFAS – global ensemble streamflow forecasting and flood early warning." *Earth Syst. Sci.* 17: 1161–1175. http://dx.doi.org/doi:10.5194/hess-17-1161-2013.

Alfieri, L., P. Salamon, A. Bianchi, J. Neal, P. Bates, and L. Feyen. 2014. "Advances in pan-European flood hazard mapping." *Hydrol. Process.* 28 (13): 4067-4077.

Alho, P., and J. Aaltonen. 2008. "Comparing a 1D hydraulic model with a 2D hydraulic model for the simulation of extreme glacial outburst floods." *Hydrol. Process.* 22 (10): 1537-1547.

Ballesteros Cánovas, J.A., M. Eguíbar, J.M. Bodoque, A. Díez-Herrero, M. Stoffel, and I. Gutiérrez-Pérez. 2011. "Estimating flash flood discharge in an ungauged mountain catchment with 2D hydraulic models and dendrogeomorphic paleostage indicators." *Hydrol. Process.* 25 (6): 970–979.

Bates, P.D., and A.P.J De Roo. 2000. "A simple raster-based model for flood inundation simulation." *J. Hydrol.* 236 (1-2): 54-77.

Bates, P.D., K. Marks, and M.S. Horritt. 2003. "Optimal use of high-resolution topographic data in flood inundation models." *Hydrol. Process.* 17 (3): 537-557.

Bates, P.D., M.S. Horritt, and Timothy J. Fewtrell. 2010. "A simple inertial formulation of the shallow water equations for efficient two-dimensional flood inundation modelling." *J. Hydrol.* 387 (1-2): 33–45. http://dx.doi.org/10.1016/j.jhydrol.2010.03.027.

Begnudelli, L., and B.F. Sanders. 2007. "Simulation of the St. Francis Dam-Break Flood." *J. of Eng. Mech.* (ASCE) 133 (11).

Benjankar, R., D. Tonina, and J. McKean. 2014. "One-dimensional and two-dimensional hydrodynamic modeling derived flow properties: impacts on aquatic habitat quality predictions." *Earth. Surf. Process. Land.* http://dx.doi.org/10.1002/esp.3637.

Bierkens, M.F.P., V.A. Bell, P. Burek, N. Chaney, L.E. Condon, C.H. David, A. de Roo, et al. 2015. "Hyper-resolution global hydrological modelling: what is next?" *Hydrol. Process.* 29: 310-320. http://dx.doi.org/doi:10.1002/hyp.10391.

Brunner, G. W. 2014. "Combine 1D and 2D Modeling with HEC-RAS." USACE-HEC.

Buchmiller, R.C., and Eash, D.A. 2010. "Floods of May and June 2008 in Iowa: U.S. Geological Survey Open-File Report 2010–1096." 10 p.

Congalton, R.G., and K. Green. 2008. *Assessing the Accuracy of Remotely Sensed Data: Principles and Practices.* Second Edition. CRC Press - Technology & Engineering.

Cook, A., and V. Merwade. 2009. "Effect of topographic data, geometric configuration and modeling approach on flood inundation mapping." *J. Hydrol.* 377: 131–142. http://dx.doi.org/doi:10.1016/j.jhydrol.2009.08.015.

FEMA. 2008. "Flood Insurance Study, Benton County , Iowa and Incorporated Areas." Federal Emergency Management Agency, Flood Insurance.

FEMA. 2014. "Flood Insurance Study, Floyd County , Iowa and Incorporated Areas." Federal Emergency Management Agency, Flood Insurance.

FEMA. 2010. "Flood Insurance Study, Linn County , Iowa and Incorporated Areas. ." Federal Emergency Management Agency, Flood Insurance.

FEMA. 2013. "Flood Insurance Study, Mower County , Minnesota and Incorporated Areas." Federal Emergency Management Agency, Flood Insurance.

FEMA. 2014. "Flood Insurance Study, Volume 1 of 2, Tuscaloosa County, Alabama and Incorporated Areas."

FEMA. 2015. "Policy for Use of Hydrologic Engineering Center-River Analysis System in the National Flood Insurance Program." Available online at https://www.fema.gov/policy-use-hydrologic-engineering-center-river-analysis-system-national-flood-insurance-program. Last accessed on May 8, 2017.

Follum, M.L. 2012. "AutoRoute Rapid Flood Inundation Model. Coastal and Hydraulics Engineering Technical Note ERDC/CHL CHETN-IV-88. U.S. Army Engineer Research and Development Center, Coastal and Hydraulics Laboratory, Vicksburg, Mississippi."

Follum, M.L., A.A. Tavakoly, J.D. Niemann, and A.D. Snow. 2017. "AutoRAPID: A Model for Prompt Streamflow Estimation and Flood Inundation Mapping over Regional to Continental Extents." *J. Am. Water. Resour. As. (JAWRA)* 53 (2): 280-299.

Fread, D.L. 1998. "NWS FLDWAV model: Theoretical Description Hydrologic research Laboratory, Office of Hydrology, National Weather Service, NOAA."

Froehlich, David C. 1989. "Local scour at bridge abutments." *Proceedings of the 1989 National Conference on Hydraulic Engineering.* New Orleans, LA, USA: Publ by ASCE.

Hedgecock, T.S., and T.D. Feaster. 2007. *Magnitude and frequency of floods in Alabama, 2003:.* U.S. Geological Survey Scientific Investigations Report 2007–5204, 28p.,+ app. (available online at http://pubs.water.usgs.gov/sir2007-5204).

Hirabayashi, Y., R. Mahendran, S. Koirala, L. Konoshima, D. Yamazaki, S. Watanabe, H. Kim, and S. Kanae. 2013. "Global flood risk under climate change." *Nat. Clim. Change* 3: 816–821. http://dx.doi.org/doi:10.1038/nclimate1911.

Homer, C.G., J.A. Dewitz, L. Yang, S. Jin, P. Danielson, G. Xian, J. Coulston, N.D. Herold, J.D. Wickham, and K. Megown. 2015. "Completion of the 2011 National Land Cover Database for the conterminous United States-Representing a decade of land cover change information." *Photogramm. Eng. Rem. S.* 81 (5): 345-354.

Horritt, M.S., and P. Bates. 2002. "Evaluation of 1D and 2D numerical models for predicting river flood inundation." *J. Hydrol.* 268: 87-99.

Horritt, M.S., and P.D. Bates. 2001. "Effects of spatial resolution on a raster based model of flood flow." *J. Hydrol.* 253 (1): 239-249.

Hunter, N.M., P.D. Bates, M.S. Horritt, and M.D. Wilsond. 2007. "Simple spatially-distributed models for predicting flood inundation: A review." *Geomorphology* 90 (3-4): 208–225. http://dx.doi.org/10.1016/j.geomorph.2006.10.021.

Kauffeldt, A., F. Wetterhall, F. Pappenberger, P. Salamon, and J. Thielen. 2016. "Technical review of large-scale hydrological models for implementation in operational flood forecasting schemes on continental level." *Environ. Model. Softw.* 75: 68–76. doi:10.1016/j.envsoft.2015.09.009 .

Kim, M.H., S.E. Morlock, L.D. Arihood, and J.L. Kiesler. 2011. *Observed and forecast flood-inundation mapping application—A pilot study of an eleven-mile reach of the White River, Indianapolis, Indiana:.* U.S. Geological Survey Scientific Investigations Report 2011–5138, 63 p. 3 appendixes.

Leandro, J., A.S. Chen, S. Djordjević, and D.A. Savić. 2009. "Comparison of 1D/1D and 1D/2D coupled (sewer/surface) hydraulic models for urban flood simulation." *J. Hydraul. Eng.* 135 (6): 495-504.

Liu, Y.Y., D.R. Maidment, D.G. Tarboton, X. Zheng, A. Yildirim, N.S. Sazib, and S. Wang. 2016. *A CyberGIS Approach to Generating High-resolution Height Above Nearest Drainage (HAND) Raster for National Flood Mapping* . CyberGIS 16, The Third International Conference on CyberGIS and Geospatial Data Science, Urbana, Illinois, July 24-26, http://dx.doi.org.10.13140/RG.2.2.24234.41925/1.: CyberGIS Center Technical Report, CYBERGIS-TR-2016-005.

Maidment, D.R. 2015. "A Conceptual Framework for the National Flood Interoperability Experiment." *cuahsi* 22 p. Available online at: https://www.cuahsi.org/Files/Pages/documents/13623/nfieconceptualframework_revised_feb_9.pdf (last cited on February 14, 2016). .

Maidment, D.R., M.A. Rajib, P. Lin, and E.P. (Eds.) Clark. 2016. *National Water Center Innovators Program Summer Institute Report 2016.* Technical Report 13, Consortium of

Universities for the Advancement of Hydrologic Science Inc. (CUAHSI), USA, 122p. http://dx.doi.org/10.4211/technical.20161019.

Mason, D.C., D.M. Cobby, M.S. Horritt, and P.D. Bates. 2003. "Floodplain friction parameterization in two-dimensional river flood models using vegetation heights derived from airborne scanning laser altimetry." *Hydrol. Process.* 17 (9): 1711-1732.

McKay, L., T. Bondelid, T. Dewald, J. Johnston, R. Moore, and A. Rea. 2012. "NHDPlus Version 2: User Guide., accessed Dec 2016. https://nctc.fws.gov/courses/references/tutorials/geospatial/CSP7306/Readings/NHDPlusV2_User_Guide.pdf."

Moore, M.R. 2011. *Development of a High-Resolution 1D/2D Coupled Flood Simulation of Charles City, Iowa.* Master of Science Thesis, University of Iowa. http://ir.uiowa.edu/etd/1032.

Musser, Jonathan W., and Thomas R. Dyar. 2007. *Two-dimensional flood-inundation model of the Flint River at Albany, Georgia: Atlanta, Georgia.* http://pubs.usgs.gov/sir/2007/5107/, U.S. Geological Survey Scientific Investigations Report 2007-510.

Néelz, S. 2009. *Desktop review of 2D hydraulic modelling.* Environment Agency, Bristol.

Nelson, J.M., J.P. Bennett, and S.M. Wiele. 2003. "Flow and sediment transport modeling." *Tools in Geomorphology* (John Wiley & Sons: Chichester) 539–576.

Nguyen, P., A. Thorstensen, S. Sorooshian, K. Hsu, and A. Aghakouchak. 2015a. "Flood Forecasting and Inundation Mapping Using HiResFlood-UCI and Near-Real-Time

Satellite Precipitation Data: The 2008 Iowa Flood." *American Meteorological Society* 1171-1183. http://dx.doi.org/10.1175/JHM-D-14-0212.1.

Nguyen, P., A. Thorstensena, S. Sorooshian, K. Hsu, A. AghaKouchak, B. Sanders, V. Koren, Z. Cuib, and M. Smith. 2015b. "A high resolution coupled hydrologic–hydraulic model (HiResFlood-UCI) for flash flood modeling." *J. Hydrol.* 541 (Part A): 401–420.

NOAA. 2011. *AHPS Guidline Final v3.* Debbery, under contract EA133C05CQ1048 – Task Order 35.

Nobre, A., L. Cuartas, M. Hodnett, C. Rennó, G. Rodrigues, A. Silveira, M. Waterloo, and S. Saleska. 2011. "Height Above the Nearest Drainage – a hydrologically relevant new terrain model." *J. Hydrol.* 404 (1–2): 13–29.

Paiva, R.C.D., W. Collischonn, and C.E.M. Tucci. 2011. "Large scale hydrologic and hydrodynamic modeling using limited data and a GIS based approach." *J. Hydrol.* 406: 170–181. http://dx.doi.org/10.1016/j.jhydrol.2011.06.007.

Pappenberger, F., E. Dutra, F. Wetterhall, and H.L. Cloke. 2012. "Deriving global flood hazard maps of fluvial floods through a physical model cascade." *Hydrol. Earth Syst. Sci.* 16: 4143–4156. http://dx.doi.org/10.5194/hess-16-4143-2012.

Pappenberger, F., K.J. Beven, N. M. Hunter, P. D. Bates, B. T. Gouweleeuw, J. Thielen, and A. P. J. de Roo. 2005. "Cascading model uncertainty from medium range weather forecasts (10 days) through a rainfall-runoff model to flood inundation predictions within the European Flood Forecasting System (EFFS)." *Hydrol. Earth Syst. Sci.* 9 (4): 381 – 393.

Pappenberger, F., P. Matgen, K.J. Beven, J. Henry, L. Pfister, and Paul F. de. 2006. "Influence of uncertain boundary conditions and model structure on flood inundation predictions." *Adv. Water Resour.* 29 (10): 1430-1449.

Patro, S., C. Chatterjee, and S. Mohanty. 2009. *J Indian Soc Remote Sens* 37 (107): http://dx.doi.org/10.1007/s12524-009-0002-1.

Rajib, M.A., V. Merwade, and Z. Liu. 2016. "Large scale high resolution flood inundation mapping in near real-time." *40th Anniversary of the Association of State Flood Plain Managers National Conference, Grand Rapids, Michigan, USA, 19-24 June, . Available online at: http://www.asfpmfoundation.org/ace-images/Adnan_Full2016.pdf (last cited on December 21, 2016).*

Rennó, C.D., A.D. Nobre, L.A. Cuartas, J.V. Soares, M.G. Hodnett, J. Tomasella, and M.J. Waterloo. 2008. "HAND, a new terrain descriptor using SRTM-DEM: mapping terra-firme rainforest environments in Amazonia." *Remote Sens. Environ.* 112: 3469–3481.

Rodda, H.J.E. 2005. "The Development and Application of a Flood Risk Model for the Czech Republic." *Nat. Hazards* 36 (1-2): 207–220. http://dx.doi.org/10.1007/s11069-004-4549.

RStudio: Integrated Development for R. RStudio, Inc. n.d. Boston , MA: http://www.rstudio.com/.

Sanders, B.F. 2007. "Evaluation of on-line DEMs for flood inundation modeling." *Adv. Water Resour.* 30 (8): 1831–1843. http://dx.doi.org/10.1016/j.advwatres.2007.02.005.

Schumann, G.J.-P., J.C. Neal, N. Voisin, K.M. Andreadis, F. Pappenberger, N. Phanthuwongpakdee, A.C. Hall, and P.D. Bates. 2013. "A first large-scale flood inundation forecasting model." *Water Resour. Res.* 49: 6248–6257. http://dx.doi.org/10.1002/wrcr.20521.

Snow, A.D. 2016. *AutoRoutePy: 2.1.0 [Data set]. Zenodo. http://doi.org/10.5281/zenodo.54974.*

Tavakoly, A.A, M.L. Follum, M. Wahl, and A. Snow. 2017. "Continental-Scale River Flow Modeling of the Mississippi River Basin Using High-Resolution NHDPlus Dataset." *J. Am. Water. Resour. As. (JAWRA)* 53 (2): 258-279. http://dx.doi.org/10.1111/ 1752-1688.12456.

Tayefi, V., S. Lane, R. Hardy, and D. Yu. 2007. "A comparison of one- and two-dimensional approaches to modelling flood inundation over complex upland floodplains." *Hydrol. Process.* 21: 3190-3202.

U.S. Army Corps of Engineers. June 2014. "Design Deficiency Report With Environmental Assessment, Northport Levee Repair Project ." Northport, Alabama.

Vanderkimpen, P., and E., Peeters, P. Melger. 2009. "Chapter 9. Flood modeling for risk evaluation—a MIKE FLOOD vs SOBEK 1D2D benchmark study." *Flood Risk Management: Research and Practice* (CRC Press 2008) 77–84. http://dx.doi.org/10.1201/9780203883020.ch9.

Vojinovic, Z., and D. Tutulic. 2009. "On the use of 1D and coupled 1D-2D modelling approaches for assessment of flood damage in urban areas." *Urban Water J.* 6 (3): 183-199.

Winsemius, H.C., L.P.H. Van Beek, B. Jongman, P.J. Ward, and A. Bouwman. 2013. "A framework for global river flood risk assessments." *Hydrol. Earth Syst. Sci.* 17: 1871–1892. http://dx.doi.org/10.5194/hess-17-1871-2013.

Wood, E.F., J.K. Roundy, T.J. Troy, L.P.H.v. Beek, M.F.P. Bierkens, E. Blyth, A.d. Roo, et al. 2011. "Hyperresolution global land surface modeling: Meeting a grand challenge for monitoring Earth's terrestrial water." *Water Resour. Res.* 47 (12): http://dx.doi.org/10.1029/2010WR010090.

Wright, N. G. , M.ASCE, I. Villanueva, P. D. Bates, D. C. Mason, M. D. Wilson, G. Pender, and S. Neelz. 2008. "Downloaded 59 times TECHNICAL PAPERS Case Study of the Use of Remotely Sensed Data for Modeling Flood Inundation on the River Severn, U.K." *J. of Hydraul. Eng.* (ASCE) 134 (5).

Yu, D., and S. N. Lane. 2006. "Urban fluvial flood modelling using a two-dimensional diffusion-wave treatment, part 2: development of a sub-grid-scale treatment." *Hydrol. Process.* 20: 1567–1583.

Zheng, X., P. Lin, S. Keane, C. Kesler, and M.A. Rajib. 2016. *"NHDPlus-HAND evaluation". In Maidment et al. (Eds.), National Water Center Innovators Program Summer Institute Report 2016.* Technical Report 13, Consortium of Universities for the Advancement of Hydrologic Science Inc. (CUAHSI), USA, pp. 26-36. http://dx.doi.org/10.4211/technical.20161019.

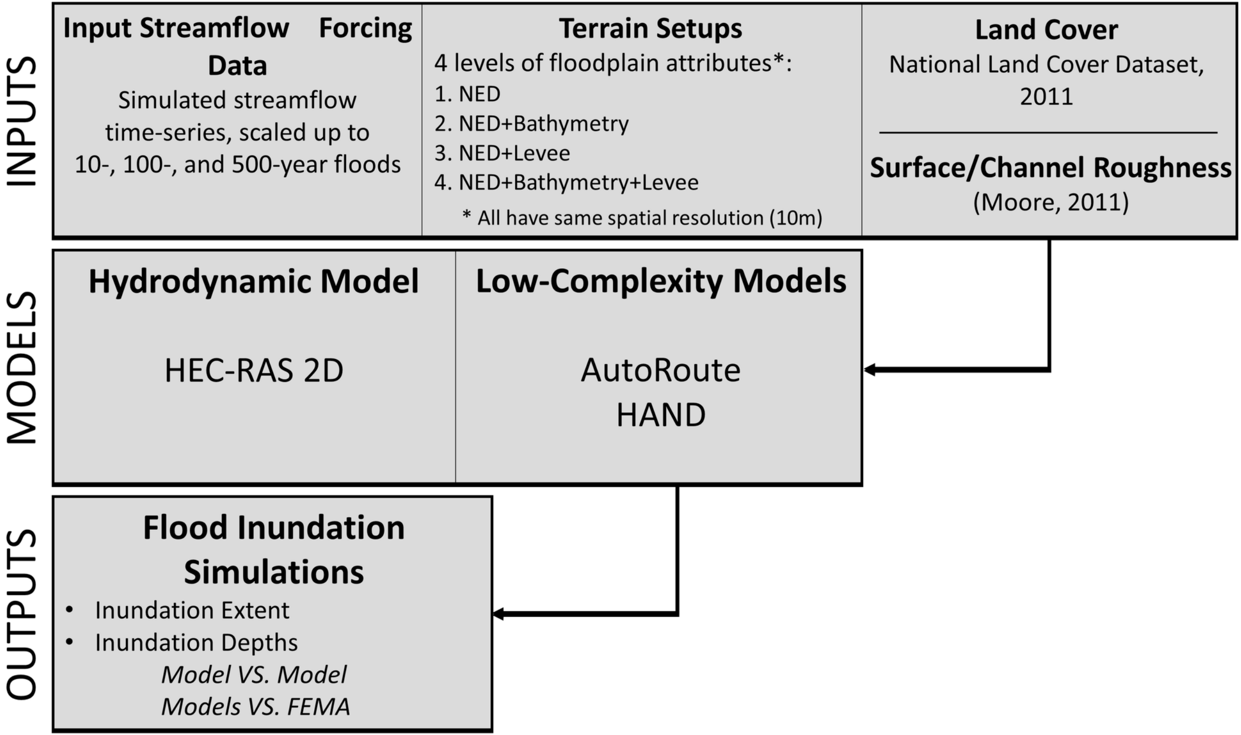
INPUTS
Input Streamflow Forcing Data
Simulated streamflow time-series, scaled up to 10-, 100-, and 500-year floods
Terrain Setups
4 levels of floodplain attributes*:
1. NED
2. NED+Bathymetry
3. NED+Levee
4. NED+Bathymetry+Levee
* All have same spatial resolution (10m)
Land Cover
National Land Cover Dataset, 2011
Surface/Channel Roughness
(Moore, 2011)
MODELS
Hydrodynamic Model
HEC-RAS 2D
Low-Complexity Models
AutoRoute
HAND
OUTPUTS
Flood Inundation Simulations
Inundation Extent
Inundation Depths
Model VS. Model
Models VS. FEMA

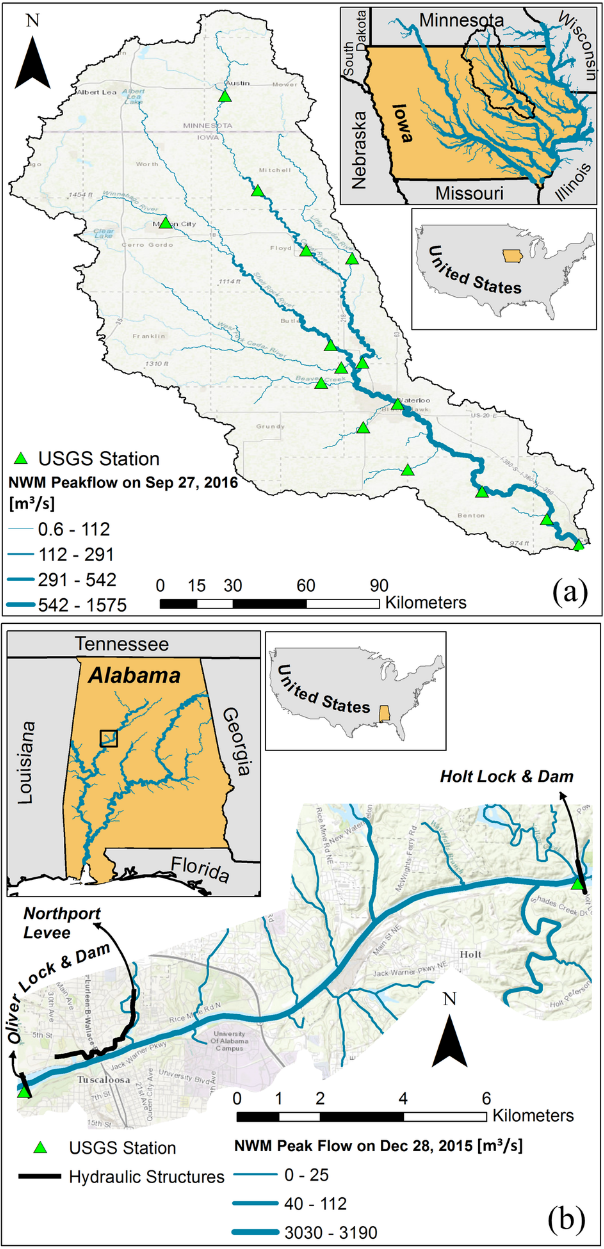

N
Minnesota
South Dakota
Wisconsin
Iowa
Nebraska
Missouri
Illinois
United States
Austin
Albert Lea
Mitchell
Floyd
Cerro Gordo
Worth
Franklin
Butler
Waterloo
Black Hawk
Grundy
Benton
USGS Station
NWM Peakflow on Sep 27, 2016 [m³/s]
0.6 - 112
112 - 291
291 - 542
542 - 1575
0 15 30 60 90 Kilometers
(a)
Tennessee
Alabama
Louisiana
Georgia
Florida
United States
Holt Lock & Dam
Northport Levee
Oliver Lock & Dam
Holt
Tuscaloosa
University Of Alabama Campus
N
0 1 2 4 6 Kilometers
USGS Station
Hydraulic Structures
NWM Peak Flow on Dec 28, 2015 [m³/s]
0 - 25
40 - 112
3030 - 3190
(b)

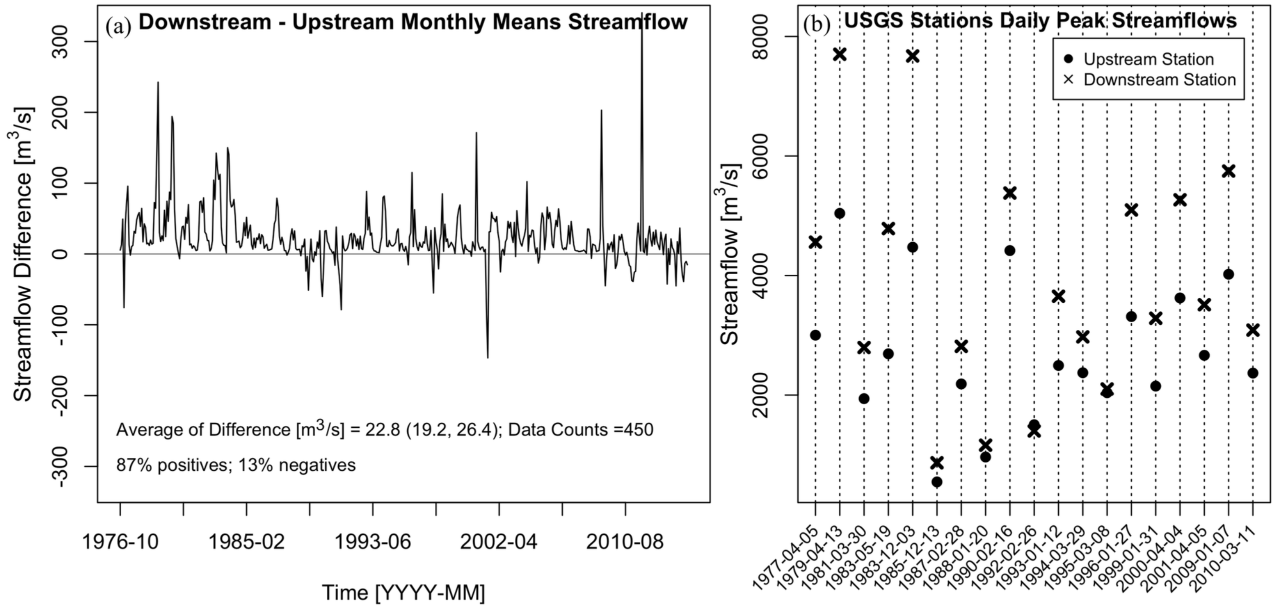
(a) Downstream - Upstream Monthly Means Streamflow
Streamflow Difference [m3/s]
Time [YYYY-MM]
Average of Difference [m3/s] = 22.8 (19.2, 26.4); Data Counts =450
87% positives; 13% negatives
(b) USGS Stations Daily Peak Streamflows
Streamflow [m3/s]
Upstream Station
Downstream Station

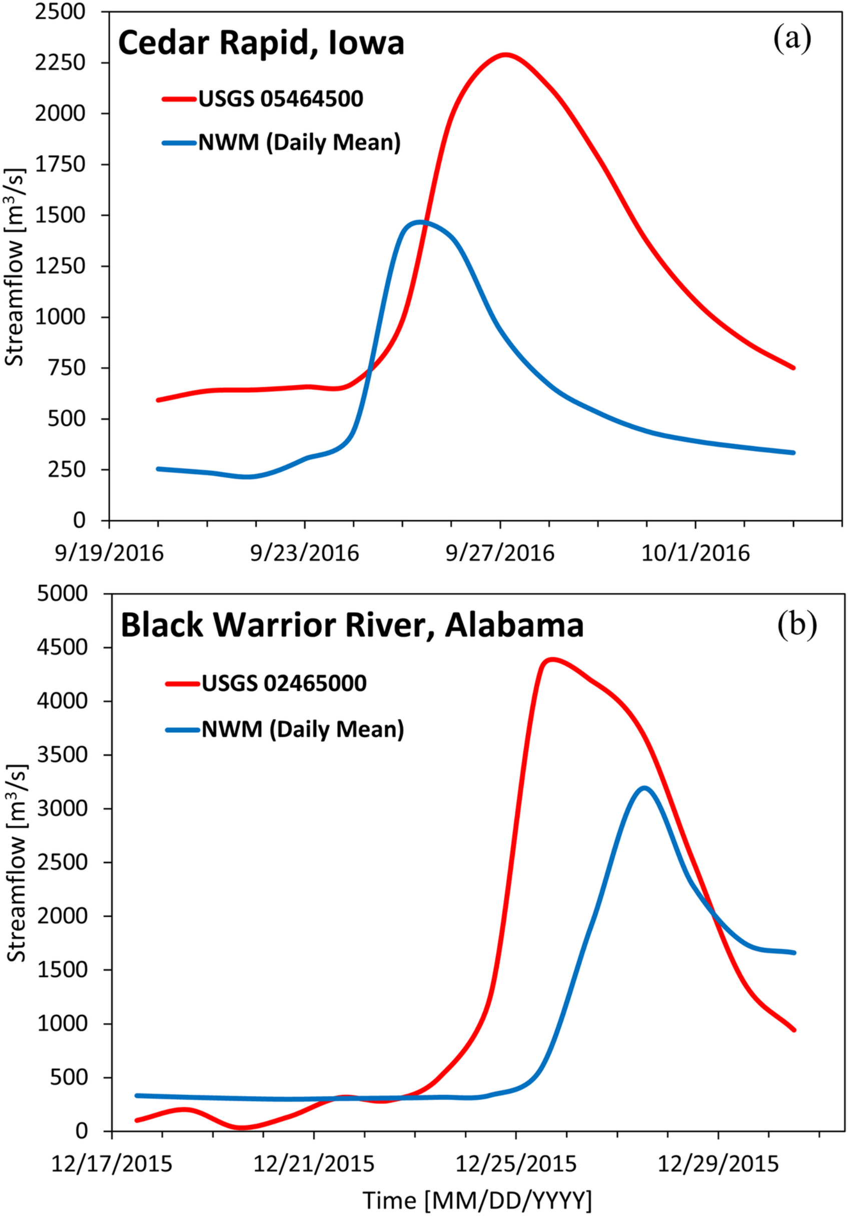

Cedar Rapid, Iowa
(a)
USGS 05464500
NWM (Daily Mean)
Streamflow [m3/s]
2500
2250
2000
1750
1500
1250
1000
750
500
250
0
9/19/2016
9/23/2016
9/27/2016
10/1/2016
Black Warrior River, Alabama
(b)
USGS 02465000
NWM (Daily Mean)
Streamflow [m3/s]
5000
4500
4000
3500
3000
2500
2000
1500
1000
500
0
12/17/2015
12/21/2015
12/25/2015
12/29/2015
Time [MM/DD/YYYY]

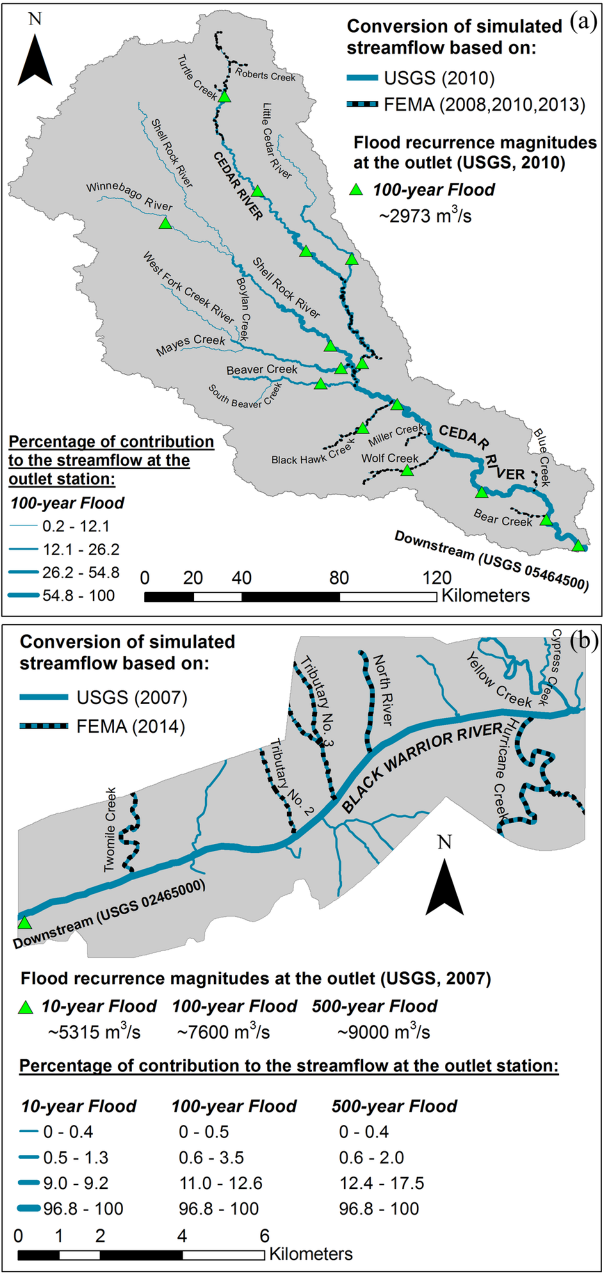

(a)
N
Conversion of simulated streamflow based on:
USGS (2010)
FEMA (2008,2010,2013)
Flood recurrence magnitudes at the outlet (USGS, 2010)
100-year Flood
~2973 m3/s
Turtle Creek
Roberts Creek
Little Cedar River
Shell Rock River
CEDAR RIVER
Winnebago River
West Fork Creek River
Boylan Creek
Shell Rock River
Mayes Creek
Beaver Creek
South Beaver Creek
Black Hawk Creek
Miller Creek
Wolf Creek
CEDAR RIVER
Blue Creek
Bear Creek
Downstream (USGS 05464500)
Percentage of contribution to the streamflow at the outlet station:
100-year Flood
0.2 - 12.1
12.1 - 26.2
26.2 - 54.8
54.8 - 100
0 20 40 80 120 Kilometers
(b)
Conversion of simulated streamflow based on:
USGS (2007)
FEMA (2014)
Tributary No. 3
North River
Yellow Creek
Cypress Creek
Tributary No. 2
BLACK WARRIOR RIVER
Hurricane Creek
Twomile Creek
N
Downstream (USGS 02465000)
Flood recurrence magnitudes at the outlet (USGS, 2007)
10-year Flood 100-year Flood 500-year Flood
~5315 m3/s ~7600 m3/s ~9000 m3/s
Percentage of contribution to the streamflow at the outlet station:
10-year Flood 100-year Flood 500-year Flood
0 - 0.4 0 - 0.5 0 - 0.4
0.5 - 1.3 0.6 - 3.5 0.6 - 2.0
9.0 - 9.2 11.0 - 12.6 12.4 - 17.5
96.8 - 100 96.8 - 100 96.8 - 100
0 1 2 4 6 Kilometers

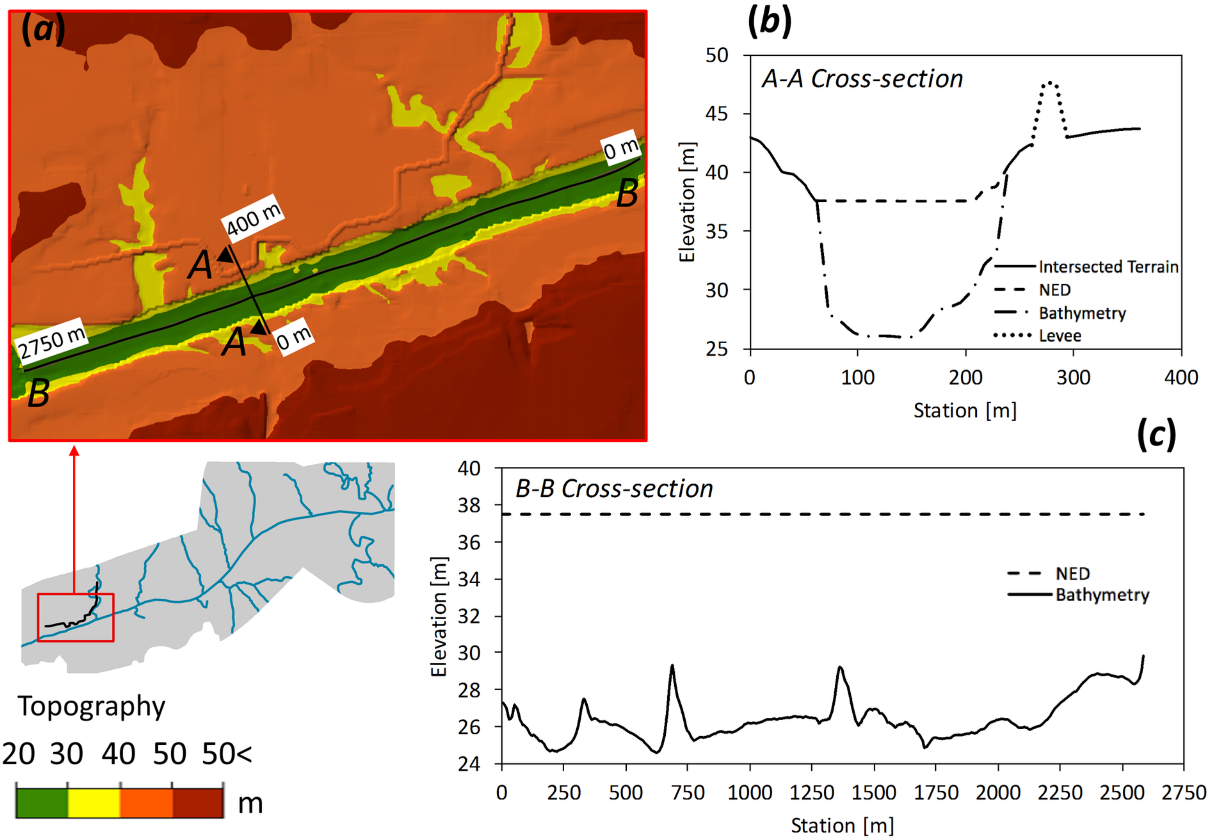

(a)
400 m
0 m
2750 m
A
A
B
B
Topography
20 30 40 50 50<
m
(b)
A-A Cross-section
Elevation [m]
Station [m]
Intersected Terrain
NED
Bathymetry
Levee
50
45
40
35
30
25
0
100
200
300
400
(c)
B-B Cross-section
Elevation [m]
Station [m]
NED
Bathymetry
40
38
36
34
32
30
28
26
24
0
250
500
750
1000
1250
1500
1750
2000
2250
2500
2750

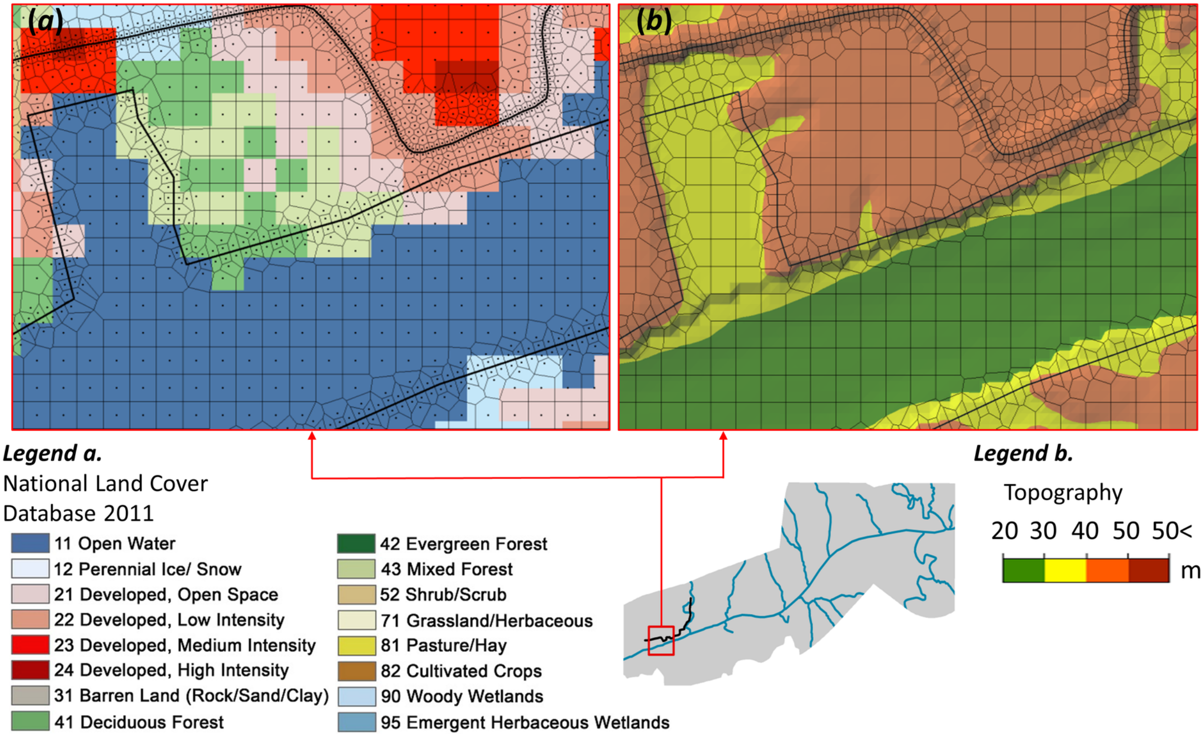
(a)
(b)
Legend a.
National Land Cover
Database 2011
11 Open Water
12 Perennial Ice/ Snow
21 Developed, Open Space
22 Developed, Low Intensity
23 Developed, Medium Intensity
24 Developed, High Intensity
31 Barren Land (Rock/Sand/Clay)
41 Deciduous Forest
42 Evergreen Forest
43 Mixed Forest
52 Shrub/Scrub
71 Grassland/Herbaceous
81 Pasture/Hay
82 Cultivated Crops
90 Woody Wetlands
95 Emergent Herbaceous Wetlands
Legend b.
Topography
20 30 40 50 50<
m

		Inundation Model 2		
		w2	d2	
Inundation Model 1	w1	$n_{w1,w2}$	$n_{w1,d2}$	$n_{w1,w2+d2}$
	d1	$n_{d1,w2}$	$n_{d1,d2}$	$n_{d1,w2+d2}$
		$n_{w1+d1,w2}$	$n_{w1+d1,d2}$	n

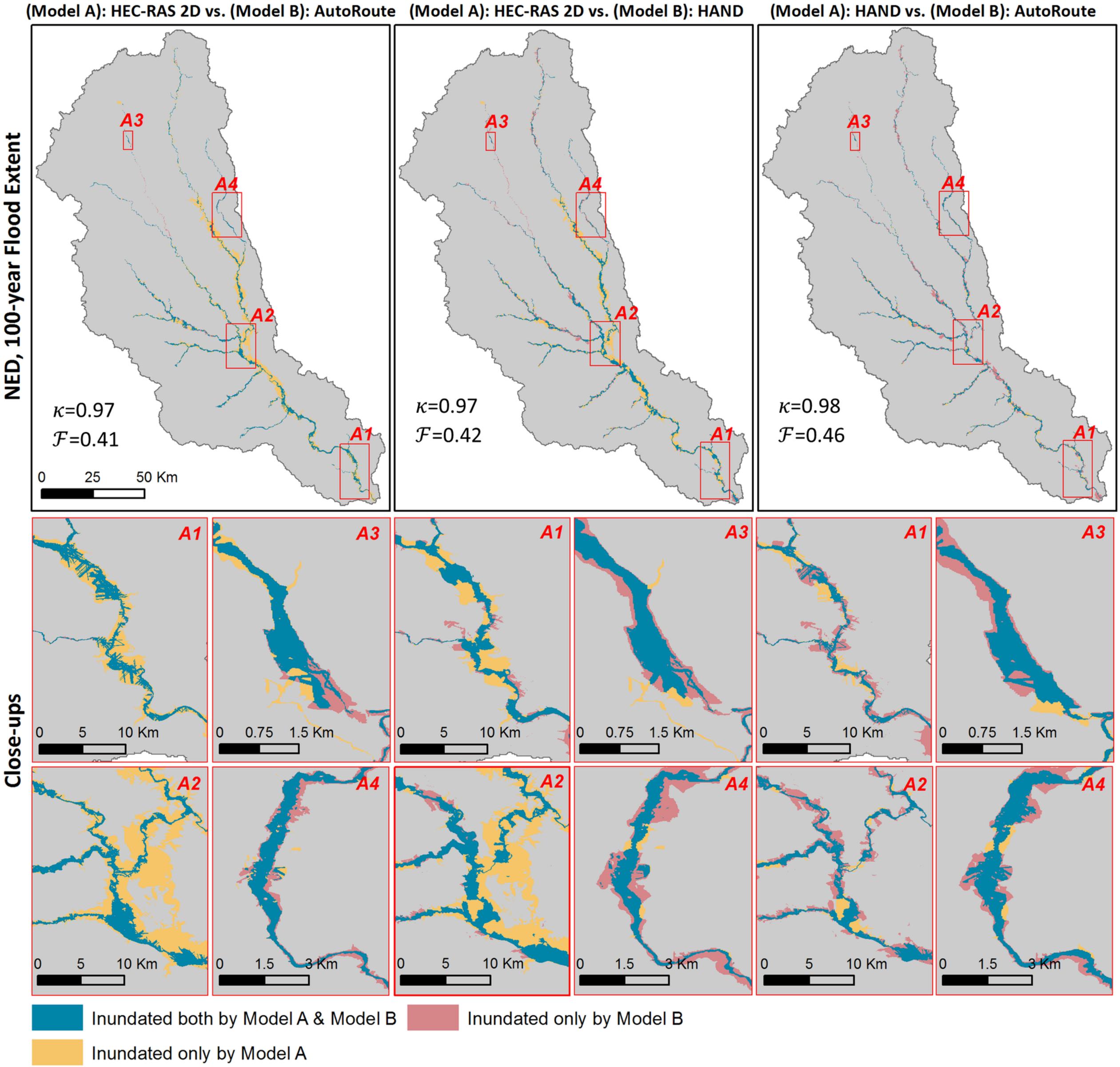
(Model A): HEC-RAS 2D vs. (Model B): AutoRoute
(Model A): HEC-RAS 2D vs. (Model B): HAND
(Model A): HAND vs. (Model B): AutoRoute
NED, 100-year Flood Extent
A1
A2
A3
A4
κ=0.97
ℱ=0.41
κ=0.97
ℱ=0.42
κ=0.98
ℱ=0.46
0 25 50 Km
Close-ups
0 5 10 Km
0 0.75 1.5 Km
0 1.5 3 Km
Inundated both by Model A & Model B
Inundated only by Model B
Inundated only by Model A

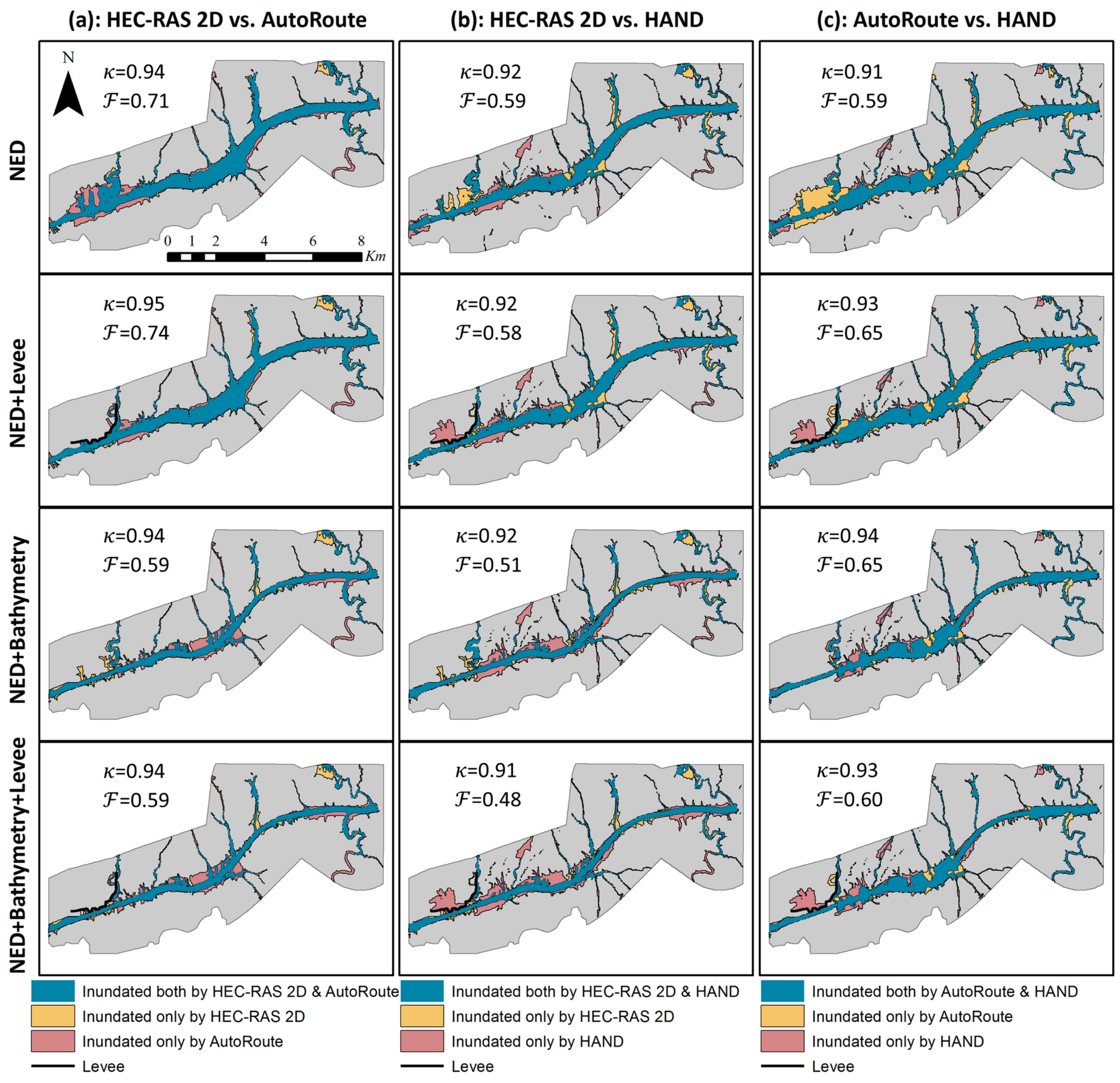
(a): HEC-RAS 2D vs. AutoRoute
(b): HEC-RAS 2D vs. HAND
(c): AutoRoute vs. HAND
NED
NED+Levee
NED+Bathymetry
NED+Bathymetry+Levee
N
0 1 2 4 6 8 Km
κ=0.94 𝓕=0.71
κ=0.92 𝓕=0.59
κ=0.91 𝓕=0.59
κ=0.95 𝓕=0.74
κ=0.92 𝓕=0.58
κ=0.93 𝓕=0.65
κ=0.94 𝓕=0.59
κ=0.92 𝓕=0.51
κ=0.94 𝓕=0.65
κ=0.94 𝓕=0.59
κ=0.91 𝓕=0.48
κ=0.93 𝓕=0.60
Inundated both by HEC-RAS 2D & AutoRoute
Inundated only by HEC-RAS 2D
Inundated only by AutoRoute
Levee
Inundated both by HEC-RAS 2D & HAND
Inundated only by HEC-RAS 2D
Inundated only by HAND
Levee
Inundated both by AutoRoute & HAND
Inundated only by AutoRoute
Inundated only by HAND
Levee

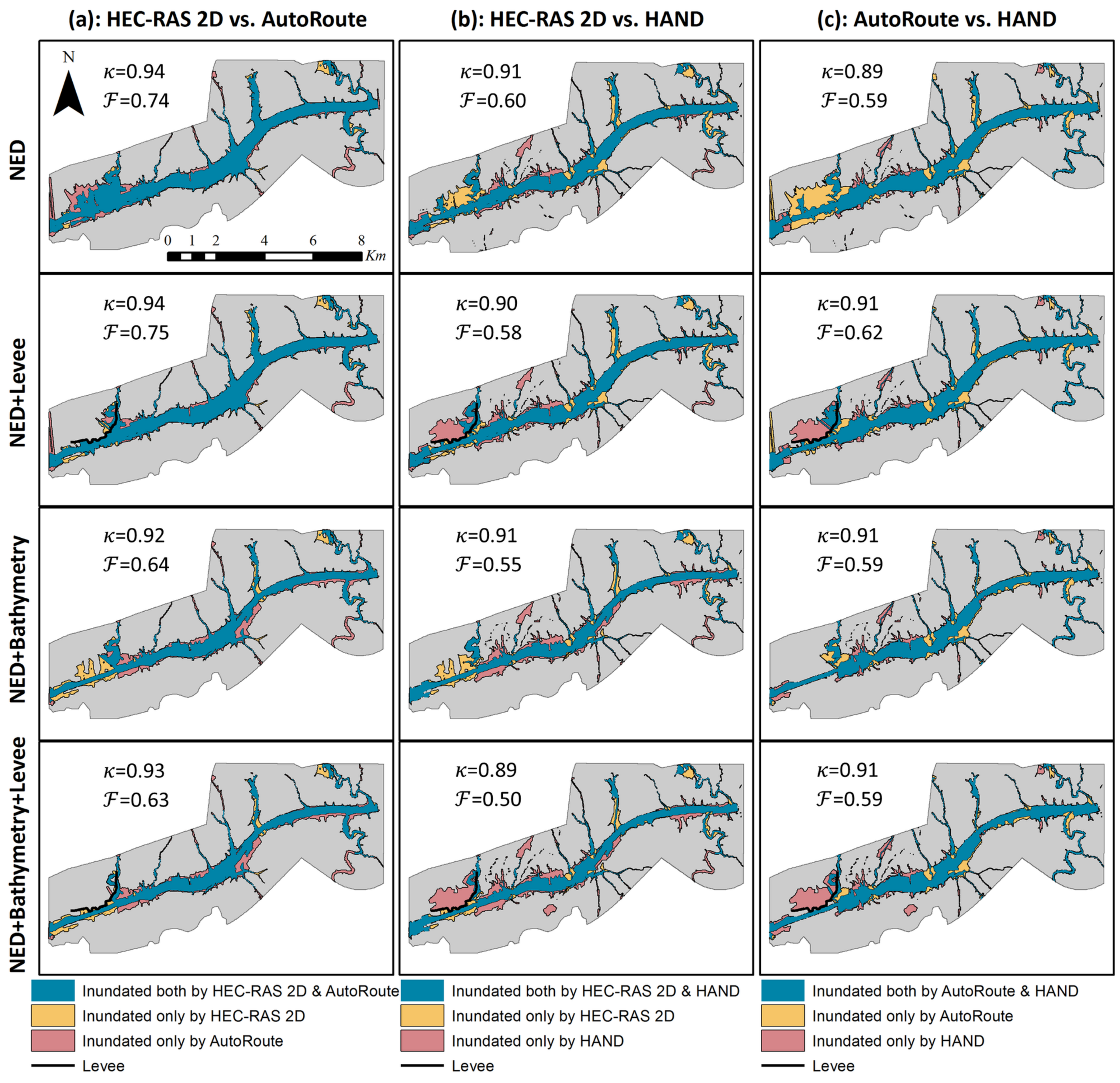
(a): HEC-RAS 2D vs. AutoRoute
(b): HEC-RAS 2D vs. HAND
(c): AutoRoute vs. HAND
NED
NED+Levee
NED+Bathymetry
NED+Bathymetry+Levee
N
0 1 2 4 6 8 Km
κ=0.94 ℱ=0.74
κ=0.91 ℱ=0.60
κ=0.89 ℱ=0.59
κ=0.94 ℱ=0.75
κ=0.90 ℱ=0.58
κ=0.91 ℱ=0.62
κ=0.92 ℱ=0.64
κ=0.91 ℱ=0.55
κ=0.91 ℱ=0.59
κ=0.93 ℱ=0.63
κ=0.89 ℱ=0.50
κ=0.91 ℱ=0.59
Inundated both by HEC-RAS 2D & AutoRoute
Inundated only by HEC-RAS 2D
Inundated only by AutoRoute
Levee
Inundated both by HEC-RAS 2D & HAND
Inundated only by HEC-RAS 2D
Inundated only by HAND
Levee
Inundated both by AutoRoute & HAND
Inundated only by AutoRoute
Inundated only by HAND
Levee

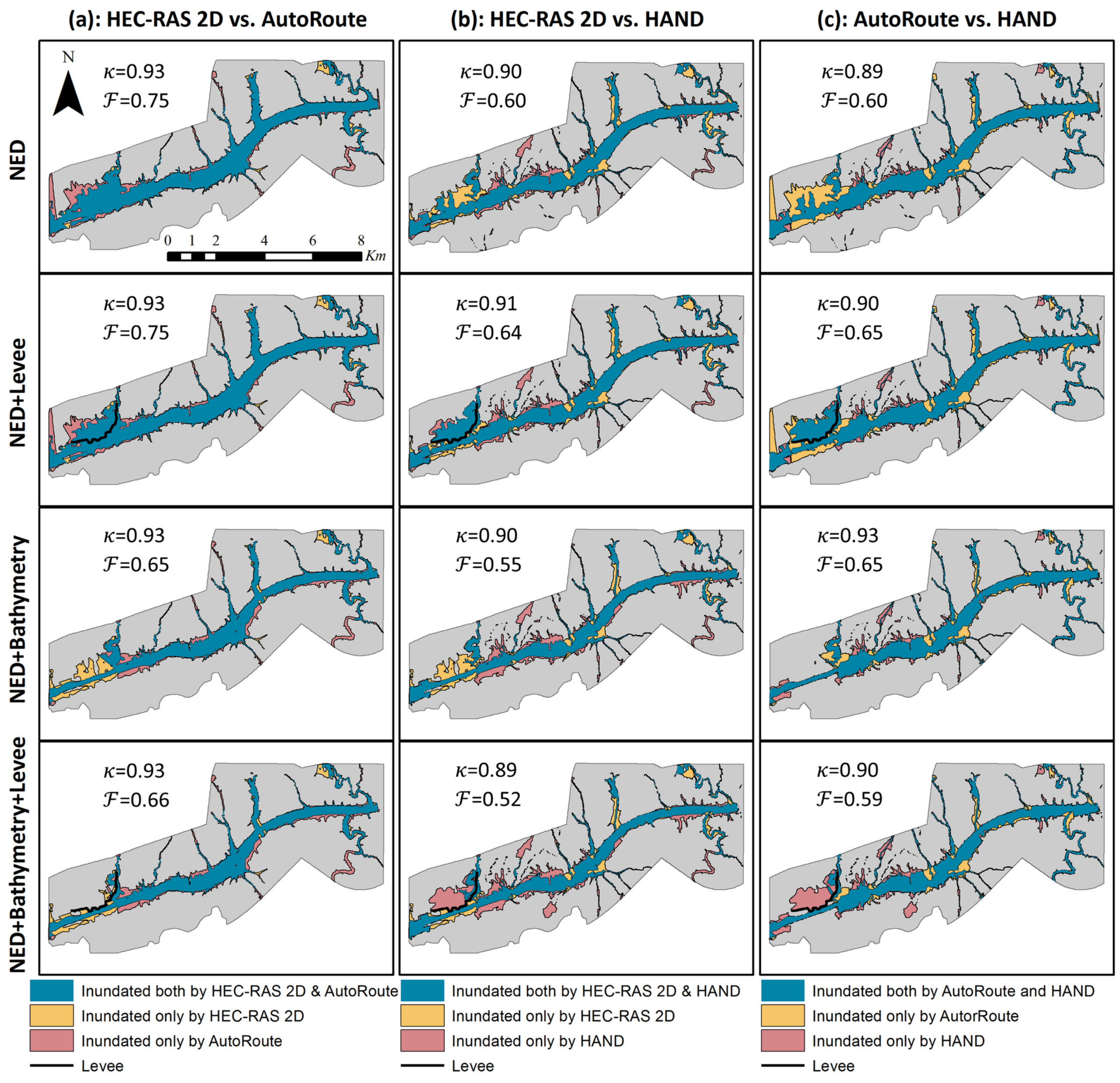

(a): HEC-RAS 2D vs. AutoRoute
(b): HEC-RAS 2D vs. HAND
(c): AutoRoute vs. HAND
NED
NED+Levee
NED+Bathymetry
NED+Bathymetry+Levee
N
0 1 2 4 6 8
Km
κ=0.93
ℱ=0.75
κ=0.90
ℱ=0.60
κ=0.89
ℱ=0.60
κ=0.93
ℱ=0.75
κ=0.91
ℱ=0.64
κ=0.90
ℱ=0.65
κ=0.93
ℱ=0.65
κ=0.90
ℱ=0.55
κ=0.93
ℱ=0.65
κ=0.93
ℱ=0.66
κ=0.89
ℱ=0.52
κ=0.90
ℱ=0.59
Inundated both by HEC-RAS 2D & AutoRoute
Inundated only by HEC-RAS 2D
Inundated only by AutoRoute
Levee
Inundated both by HEC-RAS 2D & HAND
Inundated only by HEC-RAS 2D
Inundated only by HAND
Levee
Inundated both by AutoRoute and HAND
Inundated only by AutorRoute
Inundated only by HAND
Levee

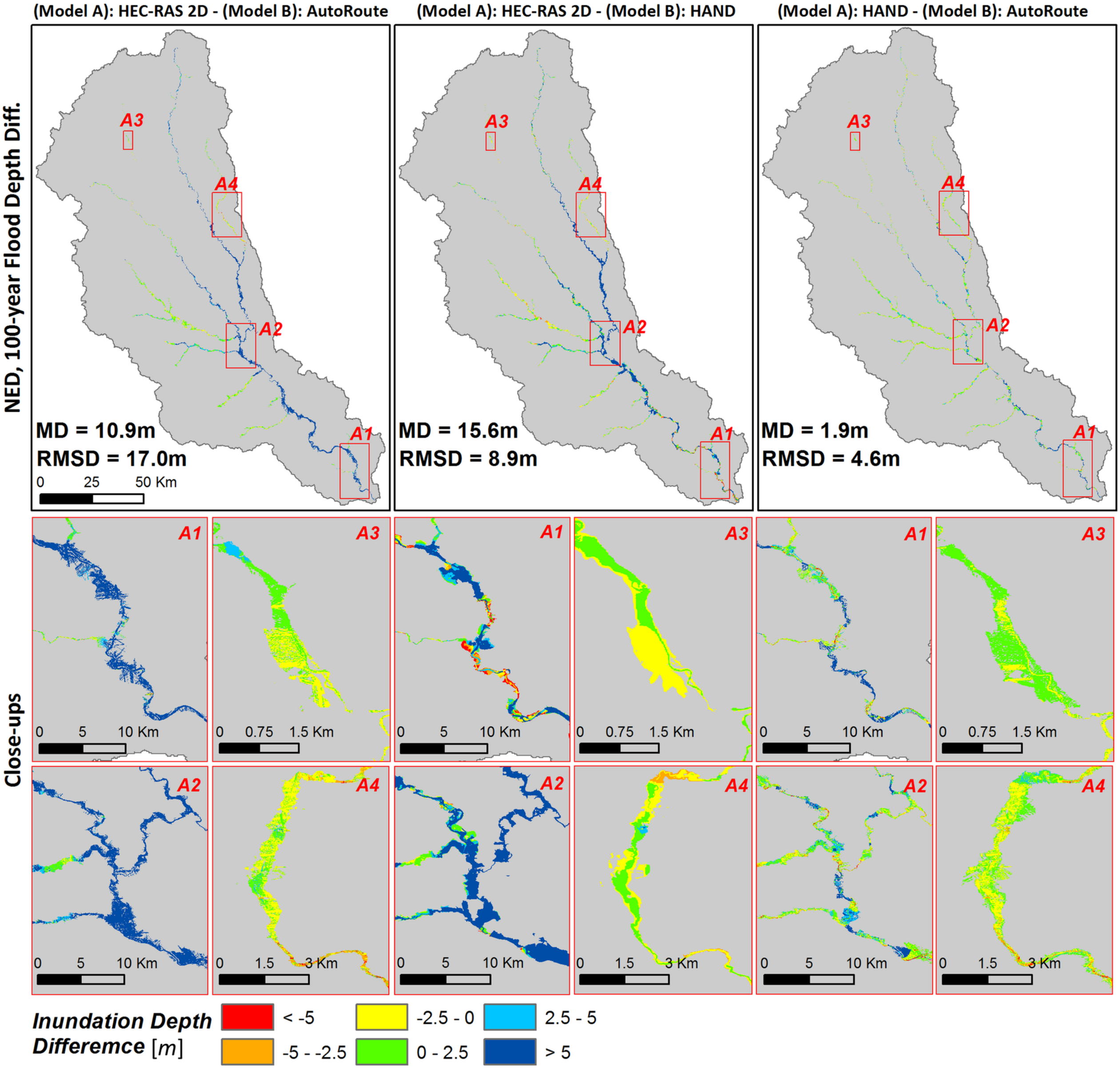
(Model A): HEC-RAS 2D - (Model B): AutoRoute
(Model A): HEC-RAS 2D - (Model B): HAND
(Model A): HAND - (Model B): AutoRoute
NED, 100-year Flood Depth Diff.
MD = 10.9m
RMSD = 17.0m
MD = 15.6m
RMSD = 8.9m
MD = 1.9m
RMSD = 4.6m
A1
A2
A3
A4
0 25 50 Km
Close-ups
0 5 10 Km
0 0.75 1.5 Km
0 1.5 3 Km
Inundation Depth Differemce [m]
< -5
-5 - -2.5
-2.5 - 0
0 - 2.5
2.5 - 5
> 5

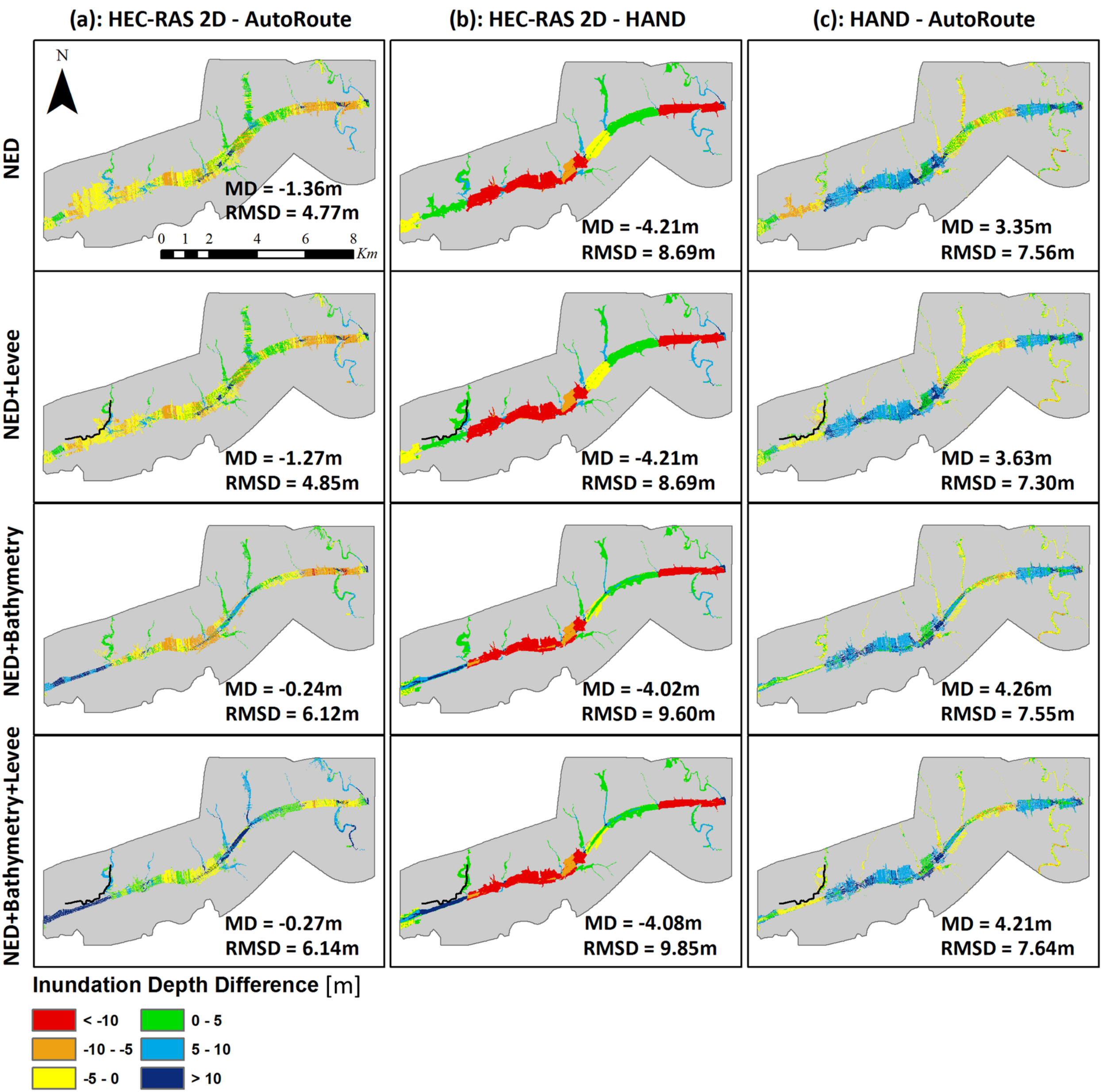

(a): HEC-RAS 2D - AutoRoute
(b): HEC-RAS 2D - HAND
(c): HAND - AutoRoute
NED
NED+Levee
NED+Bathymetry
NED+Bathymetry+Levee
N
0 1 2 4 6 8 Km
MD = -1.36m
RMSD = 4.77m
MD = -4.21m
RMSD = 8.69m
MD = 3.35m
RMSD = 7.56m
MD = -1.27m
RMSD = 4.85m
MD = -4.21m
RMSD = 8.69m
MD = 3.63m
RMSD = 7.30m
MD = -0.24m
RMSD = 6.12m
MD = -4.02m
RMSD = 9.60m
MD = 4.26m
RMSD = 7.55m
MD = -0.27m
RMSD = 6.14m
MD = -4.08m
RMSD = 9.85m
MD = 4.21m
RMSD = 7.64m
Inundation Depth Difference [m]
< -10
-10 - -5
-5 - 0
0 - 5
5 - 10
> 10

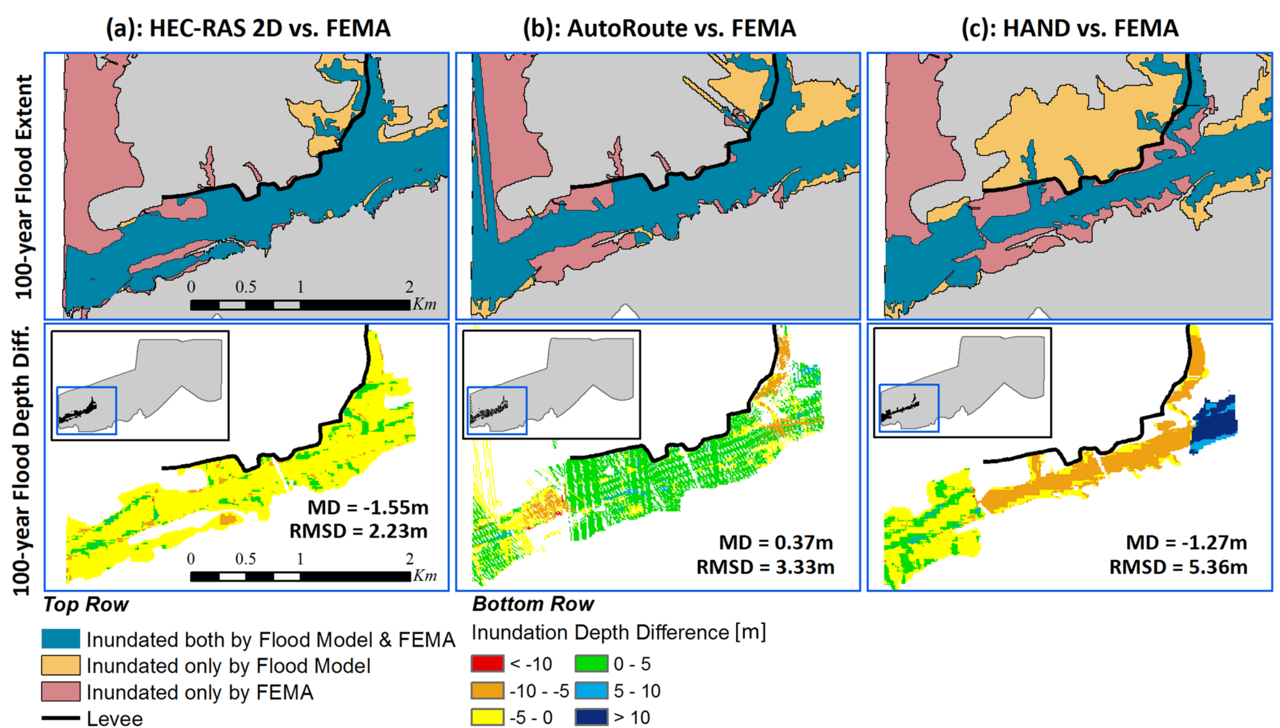
(a): HEC-RAS 2D vs. FEMA
(b): AutoRoute vs. FEMA
(c): HAND vs. FEMA
100-year Flood Extent
100-year Flood Depth Diff.
0 0.5 1 2 Km
MD = -1.55m
RMSD = 2.23m
MD = 0.37m
RMSD = 3.33m
MD = -1.27m
RMSD = 5.36m
Top Row
Inundated both by Flood Model & FEMA
Inundated only by Flood Model
Inundated only by FEMA
Levee
Bottom Row
Inundation Depth Difference [m]
< -10
-10 - -5
-5 - 0
0 - 5
5 - 10
> 10

Table 1. Existing models being applied by researchers and flood modeling communities along with those applied in current study.

	Model	Reference(s)	Developer(s)
1	FESWMS-2DH (Finite Element Surface Water Modeling System for 2D flow in the Horizontal plane	Froehlich, D.C., 1989; Musser et al., 2007	US Geological Survey
2	FaSTMECH (Flow and Sediment Transport with Morphological Evolution of Channels)	Kim et al., 2011; Nelson et al., 2003	
3	MIKE 11 1D, MIKE 21 2D and MIKE FLOOD 1D/2D coupled hydrodynamic suit of models	Ballesteros et al., 2011; Patro et al., 2009; Wright et al., 2008	The Danish Hydraulic Institute
4	SOBEK 1D/2D	Vanderkimpen et al., 2009	Deltares-Delft Hydraulics
5	BreZo/ HiResFlood	Begnudelli and Sanders, 2007; Nguyen et al., 2015a,b; Sanders, 2007	University of California, Irvine, US
6	FLDWAV (Flood Wave Dynamic Model)	Fread, 1998	US National Weather Service
7	HEC-RAS (Hydrologic Engineering Center-River Analysis System) 1D	USACE, 2010	US Army Corps of Engineers
8	HEC-RAS (Hydrologic Engineering Center-River Analysis System) 2D *	Brunner et al., 2014	
9	LISFLOOD-FP	Alfieri et al., 2014; Bates and De Roo, 2000; Bates et al., 2010; Rajib et al., 2016; Schumann et al., 2013	University of Bristol, UK
10	AutoRoute *	Follum, 2012; Follum et al., 2017	US Army Corps of Engineers
11	HAND (Height Above the Nearest Drainage) for continental US *	Maidment et al. (2016); Zheng et al., 2016	Liu et al., 2016

* Models being applied and tested in current study

Table 2. Configurations for multi-model comparison. Each of the three models used in this study had 13 configurations as listed below.

Configuration	**Flood event (return period)**	**Terrain setup**			**Testbed**
		NED	Bathymetry	Levee	
1	10-year	10 m	×	×	
2			√	×	
3			×	√	
4			√	√	
5	100-year	10 m	×	×	Black Warrior River (BWR), Alabama
6			√	×	
7			×	√	
8			√	√	
9	500-year	10 m	×	×	
10			√	×	
11			×	√	
12			√	√	
13	100-year	10 m	×	×	Cedar River (CR), Iowa